Technical Report

Savage River Mine Long Plains Kinetic Trials: FINAL REPORT

A. Parbhakar-Fox, N. Fox, and S, Nascimento

University of Tasmania

Savage River Mine Long Plains Kinetic Trials

University of Tasmania

Final Report

Anita Parbhakar-Fox, Nathan Fox and Sibele Nascimento

ARC Transforming the Mining Value Chain Industrial Transformation Research Hub,
University of Tasmania

September 2018

Transforming the Mining Value Chain

Final Report –September 2018

Enquiries and additional copies:

CODES, Private Bag 79, Sandy Bay, Tas, 7001

Tel: +61 (0) 3 6226 2472

Fax: +61 (0) 3 6226 2547

www.utas.edu.au/codes

This report should be cited as:
Parbhakar-Fox, A., Fox, N., and Nascimento, S. 2018. Savage River Mine Long Plains Kinetic Trials: Final Report, ARC Industrial Transformation Research Hub for Transforming the Mine Value Chain (TMVC), University of Tasmania, Australia.

EXECUTIVE SUMMARY

Project objectives

The University of Tasmania were instructed by Grange Resources Ltd (Grange) to undertake 3-year column leach kinetic trials on waste rock materials (A, B and D type) from the Long Plains project at the Savage River Mine. The objectives of this study are as follows:

1. Evaluate the geochemical and mineralogical characteristics of the column feed material;
2. Evaluate the water quality evolved from the columns (pH and EC weekly) and metals (monthly); and
3. Record mineralogical changes periodically (i.e., every three months) to identify reaction products.

The work program commenced in August 2015, and is ongoing until 2018. Correspondence with Grange Resources (Roger Hill and Tony Ferguson) was undertaken to establish the project, followed by delivery of samples to UTAS. Mineralogical evaluations of the column feed were performed (by XRD at UTAS) before homogenising each waste type, loading the cells and starting the experiments.

Scope of work

The scope of work undertaken to satisfy the research objectives were met by: (a) consulting with staff at Grange; (b) undertaking various geochemical techniques on the samples provided by Grange; and (c) evaluating all data collected to date to provide an update on the geochemical evolution of Long Plain waste materials. This interim report describes how the cells were constructed, documents the geochemical characteristics and presents kinetic trial results from the first eighteen months. The aim of this study is to provide Grange with an indication of the acid forming potential of the waste materials, to support the development of a best practice waste management plan for the Long Plains project.

Outcomes and recommendations

1 At the end of this investigation, waste Types A, B and D are NAF (after 156 weeks of testing) when using a cut-off criterion (PAF or NAF) of pH 4.5. Measurements of the bulk mineralogy confirm an abundance of neutraliser in Type A, so it is anticipated this will remain as NAF. For Types B and D results suggest that surface passivation reactions are likely occurring (enhanced by the presence of chlorite), and therefore will also likely remain NAF. Type B's neutralising properties will be enhanced if blended with Type A. Pyrite in Type D is larger in diameter and is encapsulated in silicates, it is likely that even on exposure it will remain NAF as the passivating layers appear to form quickly. Further investigations into the nature of the passivating layers and experiments to test their longevity are recommended to confirm their durability.

2 Further research investigations are being conducted outside of this project (with the University of Cape Town and Petrolab UK Ltd.) where the size fraction examinations of pyrite texture are being studied and a new biokinetic test. The results of these will be given to Grange Resources when finalised as this may be of use when planning future waste characterisation works.

TABLE OF CONTENTS

ACKNOWLEDGMENTS

Roger Hill and Tony Ferguson are thanked for their support and funding of this project, as well as organising the sample materials, and providing the appropriate background data. Daniel Lester is also thanked for initiating this project. Helen Scott (TMVC Hub, UTAS) and Caroline Burbury (UTAS) are thanked for handing all contracts and overall project management. Sibele Nascimento and Laura Jackson are thanked for irrigating the samples and taking the geochemical measurements weekly and filtering samples for solution ICP-MS analyses. Troy Finearty is thanked for organising the samples to be sent to ALS for geochemical analyses and Dr Ashley Townsend at the Central Science Laboratory for analysing the final 6-months' worth of leachates on the ICP-MS.

INTRODUCTION

1.1 Project overview

The University of Tasmania was engaged by Grange Resources assess the long-term geochemical behaviour of waste rock materials from their Long Plains exploration project, at the Savage River Mine (Figure 1). To date, 143 samples have been subject to static testwork, from which a waste model was developed. However, no kinetic testwork has been performed on these materials. Materials representative of A, B and D waste types have been identified, and are classified as acid consuming/non-acid forming, non-acid forming and potentially acid forming/extremely acid forming respectively. The aim of this project is to confirm their geochemical behaviour, to aid the understanding of how these waste materials might behave in a physical waste rock pile.

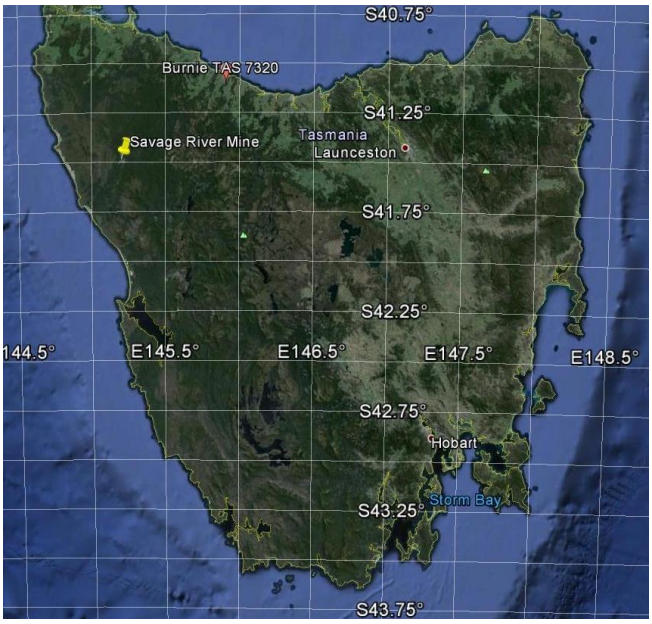

Figure 1. Location Map of Savage River mine, NW Tasmania (Image from *Google Maps*)

1.2 Savage River: waste types

Waste materials at the Savage River mine have been designated into one of four categories A to D (Table 1) based on their geochemical and mineralogical characteristics. In addition, these waste materials have been considered as having four classes of properties (I to IV) as described in Table 2.

Table 1. Savage River mine waste rock categories (GHD, 2014; Lester, *pers. comm*, 2015).

Waste class	Description
A-type	**Non-acid forming (NAF) alkaline waste rock with some level of acid neutralising capacity (ANC).** Typically, A-type contains the hard, durable, non-acid forming rocks of Type I & II. This type is intended to be used where water flow is to be encouraged to allow drainage of dump areas and to encourage alkalinity into the system.
B-type	**Neutral waste rock.** General dumping rock including all but the most reactive rocks, this particularly includes Type III rocks.
C-type	**Highly to extremely weathered, low-permeability clayey gravel.** Clay layers comprising compacted soft Type I and compacted soft Type II.
D-type	**Potentially acid forming (PAF) waste rock.** Reactive Rock - all Type IV rock and any unidentified rock types.

Table 2. Savage River mine waste rock properties.

Type	Description
I	Non Acid Forming (NAF) Carbonates, subdivided into: • Hard weather resistant & durable e.g. fresh dolomite and magnesite (estimated as 80% of total). • Soft liable to break down by weathering or compaction, e.g. weathered magnesite or dolomite (estimated as 20% of total).
II	Non Acid Forming (NAF) Non-Carbonates, subdivided into • Hard weather resistant & durable, e.g., intrusives such as gabbro, dolerite and amphibolite. • Soft liable to breakdown by weathering or compaction, e.g., eastern schist, low sulphide serpentinite and clay
III	Potentially Acid Forming (PAF) but low risk, low capacity. These materials include western schist without visible sulphide.
IV	Potentially acid forming (PAF) waste rock, These materials include volcanics, high sulphide schists, some intrusives, serpentinite, mixed waste rock and unidentified materials.

In summary, A-Type has significant alkalinity, Type-B is variable material (generally NAPP negative or neutral), Type C is non-acid forming and Type D is the most acid forming material. In this study, materials from waste types A, B and D were only submitted as Type C is considered geochemically inert in ARD terms.

1.3 Previous investigations

SGS Renison, Tasmania conducted geochemical analyses (carbon and sulphur analyses, NAG pH) on approximately 159 samples from the Long Plains exploration project. These data were used to develop a waste rock model. From these materials, ten samples were selected (by Roger Hill) for use in these kinetic trials. A summary of their geochemical characteristics is shown in Table 3. Waste Type A (n =3) is non-acid forming but may have some acid neutralising capacity. Waste Type B (n= 2) is consistently non-acid forming. Waste Type D (n= 5) shows the most diverse geochemical characteristics with classifications ranging from having neutralising capacity to extremely acid forming. In general, these materials are consistent with their expected behaviour (Table 1).

Table 3. Geochemical characteristics of the Long Plains samples used in this study.

Sample ID	Waste type	Sulphide-sulphur	MPA	ANC	NAPP	NAG pH	Classification
ABA050	D	0.3	9	206	-197	10.6	ANC
ABA051	A	0.01	0.2	941	-941	9.9	ANC
ABA052	A	0.17	5	14	-9	9.9	NAF
ABA053	A	0.01	0.2	14	-14	9	NAF
ABA054	B	0.13	4	14	-10	6.6	NAF
ABA055	B	0.44	13	14	-1	4.6	NAF
ABA056	D	0.26	8	14	-6	3.8	UC/NAF
ABA057	D	0.55	17	14	3	3.4	PAF-LC
ABA058	D	0.69	21	14	7	3	PAF-LC
ABA059	D	3.49	107	14	93	ND	EAF

1.4 Study aims

Material from each waste type was homogenised and used in long-term kinetic trials (156 weeks) to undertake the following:

- Determine the acid rock drainage characteristics of each waste type.

- Track mineralogical changes to evaluate the longevity of intrinsic neutralisation (i.e., Type A waste) and acid generation (i.e. Type D waste); and
- Assess the accuracy of the proposed waste rock model.

2.0 METHODOLOGIES

2.1 Sample receipt and preparation

Following discussions with Roger Hill and Daniel Lester in May 2015, 10 coarse samples (- 4 mm) from each waste sample were delivered to UTas (arriving in 20L buckets) in July, 2015. Each sample was weighed, with a final composite sample prepared proportionately (Table 4, Figure 2), with 2 kg samples (approximately) prepared for each waste type. All experiments were performed at UTas, unless otherwise stated.

Table 4. Observed mineralogical characteristics of the Long Plains waste samples, and their mass.

Sample ID	Waste Type	Observed minerals	Mass (g)
ABA051	A	Magnesite	599
ABA052	A	Magnesite	729
ABA053	A	Magnesite	629
ABA054	B	Chlorite, epidote	1,508
ABA055	B	Chlorite	578
ABA050	D	Chlorite, pyrite	798
ABA056	D	Chlorite, serpentinite	624
ABA057	D	Chlorite, pyrite	2,011
ABA058	D	Chlorite, pyrite	1,124
ABA059	D	Chlorite, specular hematite	1,247

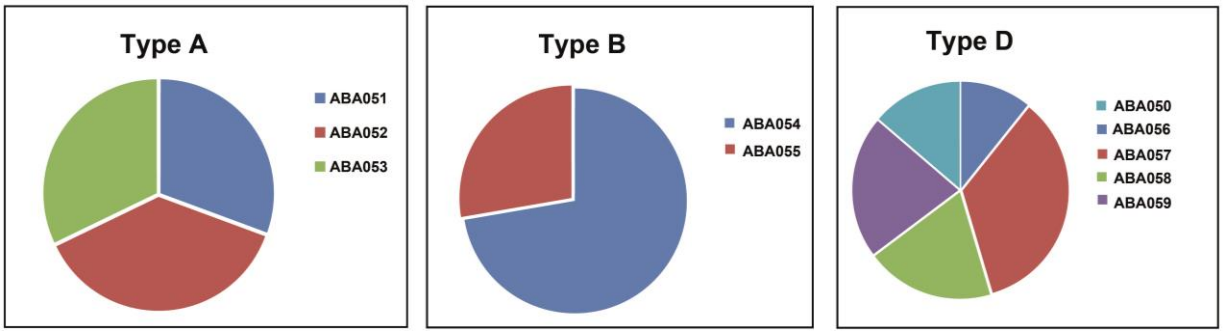

Figure 2. Ratio of each individual sample used in the preparation of kinetic trial column feed material.

2.2 Column construction and operation

The columns were prepared in accordance with the AMIRA P387A ARD Testing Handbook free draining column leach procedure (Smart et al., 2002). This methodology is the most commonly used in Australia both in research (e.g., Stewart, 2005; Miller et al. 2010; Munksgaard and Lottermoser, 2011; Parbhakar-Fox et al., 2013) and by industry as it is offered by many laboratories including ALS Global. This procedure allows flexibility in the experimental design and therefore can be modified with respect to grain size, sample mass and frequency of leachate collection. A nominal grain size of -4 mm (as recommended by the procedure) was used. In summary, each funnel was loaded with a piece of coarse 160 mm filter paper, sand (to improve drainage; 100 g) and finally waste rock (2 kg).

Four column leach tests were established in August 2015 with the -4 mm fraction fed into three columns, and one control cell (sand + filter paper) also constructed (Figure 3). Heat lamps with 150 W bulbs are recommended to maintain surface temperatures of 30 to 35°C (Smart et al., 2002). However, to accelerate oxidation, 275 W bulbs were used instead, with surface temperatures maintained at 35- 40°C. Lamps were switched on for ten hours per day for days one to five, and were switched off on days six and seven. The test solution (deionised water; DI) was applied to the surface of columns on day five; approximately two hours after heat lamps were switched off. The volume of test solution added varied as the procedure recommends to fill until the surface of material in each funnel is saturated (Smart et al., 2002). On average, approximately 500 ml was added to the columns. Leachates drained into 500 ml conical flasks at the base, which were collected weekly on day seven for geochemical assessment. Finally, these were cleaned and placed back under the Buchner funnels, and the weekly cycle repeated. A grab sample (c.10 g) was obtained from the surface of each -4 mm column every (15 weeks) for XRD analysis to provide a general indication of mineralogical changes in the column. This sample was collected on day 5 of each weekly cycle (i.e., prior to the addition of the DI water test solution), to allow for any secondary efflorescent minerals formed because of pore-water evaporation to be identified.

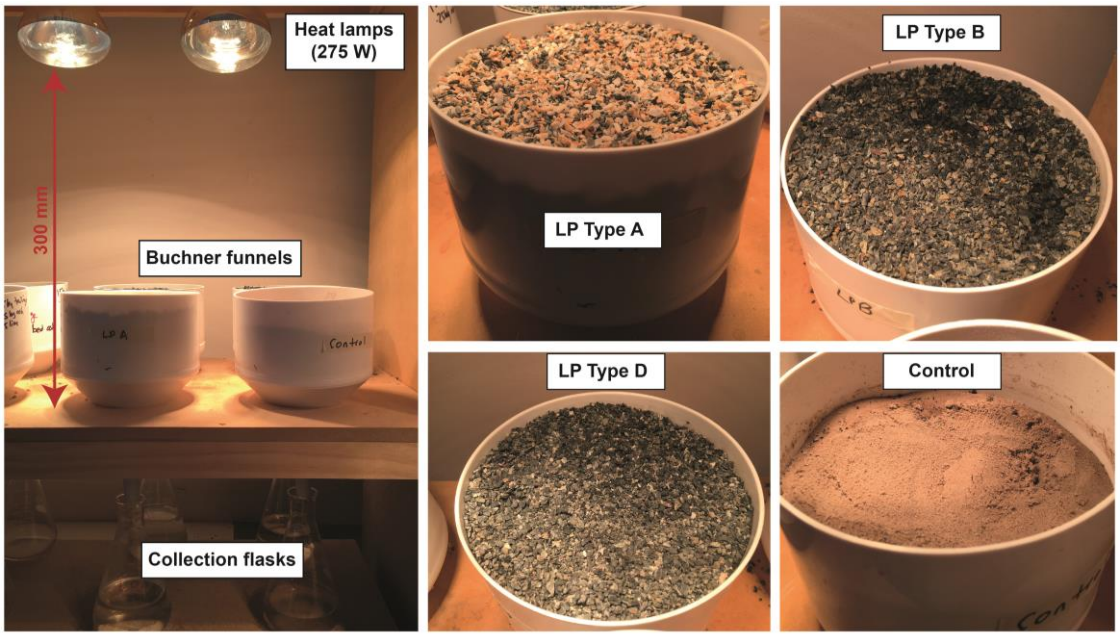

Figure 3. Kinetic trial laboratory setup, with the surface of each individual sample shown.

Each week pH and EC measurements were taken using. The pH meter (Mettler Toledo S47 SevenMulti™ dual pH/conductivity meter) was calibrated prior to use with pH 4 and 7 buffer solutions. Each measurement was taken in triplicate, and an average value calculated as the final pH. The EC meter (Euitech PC 450) was calibrated using three conductivity solutions (500, 1413 and 12.88 µS/cm-1) at 25◦ C. Every 4 weeks, the resulting liquor was filtered (0.45 µm PES Millipore filters) and 70 ml vials filled. These were refrigerated until week 26 when they were sent as a batch to ALS Global (Brisbane) for chemical analyses (Method Codes: EG020F, ED041G, EG035F) with the following elements measured: As, B, Ba, Be, Cd, Co, Cr, Cu, Hg, Mn, Ni, Pb, Se, V, Zn and SO_4. From weeks 55 to 81, Ca and Mg were also analysed to assist with tracking the rate of neutralisation. Appropriate standards and sample duplicates were used by ALS during these analyses. Samples from week 0 and

week 4 were lost by the laboratory, therefore replicate composite samples using the same waste rock ratios were made and experimented upon to obtain this data. The final six months' worth of water samples were analysed at the Central Science Laboratory (CSL), UTAS using an Element 2 HR-ICP-MS instrument. Calibration standards were made using single and multi-element analytical solutions. The major element standard (K, Fe, Al, Na, Ca, Mn and Pb) were made up to 10, 50, 100 and 10,000 ppb. Trace element standards were made up to 10, 100, 200 and 1000 ppb. Internal standards 115In (5ppm) and 185Re (5ppm) were used and added inline. The data was processed using MassHunter software from Agilent. Column feed and end of column leachates derived from NAG and paste pH testing were also analysed at UTAS using the CSL instrument.

2.3 X-ray diffractometry (XRD)

To determine the mineralogy of the column feed a split was micronised and subjected to XRD analysis. A benchtop Bruker D2 Phaser X-ray diffractometer instrument with a Co X-ray source was used to perform these analyses. Prior to the sample run, a corundum standard was analysed to check the X-ray beam alignment and ensure the correct collection of peaks. Each sample was ground in an agate pestle and mortar and loaded into the sample holder and placed into the machine chamber. Samples were analysed for 1 hour (fixed divergence slit: 1 mm; range: 4-90° 2theta; 0.02° step size, Fe-filter), with the resulting spectra proceed in Eva 2.1 software where minerals were identified using the ICDD PDF 2012 database. Patterns from all samples were then quantified using Topas 2.0 software.

2.4 Reflected light microscopy

Reflected light microscopy was performed on 3 polished laser mounts (i.e., LPA, LPB and LPD) to determine the sulphide (and magnetite) abundance and their textural associations prior to MLA- SEM analysis. An automated Nikon Eclipse LV100 microscope with DS-Ri2 imaging attachment was used for analysis at the UTAS laboratories. Prior to imaging, all sample surfaces were thoroughly cleaned with ethanol to remove skin oils and loose material.

2.5 MLA-SEM

Mineral liberation analysis was performed on the same column feed kinetic trial material (n= 3) to evaluate pyrite grain size, grain shape, and mineral associations using a FEI Quanta 600 mineral liberation analyser scanning electron microscope (MLA-SEM) at the CSL, UTAS. Grain mounts were analysed using the X-ray modal (XMOD) analyses and sparse phase liberation (SPL) method. A nickel standard was used as an internal standard. Data were processed in MLA Image Viewer to produce classified images for each sample based on a site-specific mineral library.

3.0 RESULTS

In this section, the column feed mineralogy (XRD characterisation and MLA results) and the chemical (pH, EC, metals, sulphate) results evolved over the three-year period are presented for each individual kinetic waste trial.

3.1 Waste Type A

The column feed bulk mineralogy (i.e., week 0) of type A (measured by XRD) is dominated by magnesite (32 wt. %), quartz (22 wt. %), dolomite (17 wt. %) and chlorite (10 wt. %) with only trace pyrite and magnetite reported (< 1 wt. %). Reflected light images show fine-grained pyrite and magnetite as locked in larger silicate grains (Figure 4) suggesting, in the case of pyrite, that its acid forming potential is extremely low with a net-alkaline condition expected to persist in the kinetic trial.

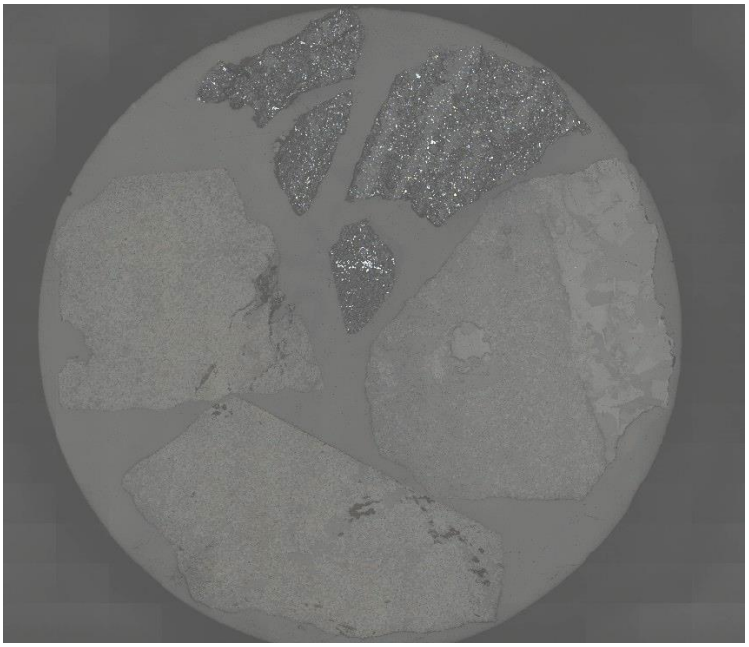

Figure 4. Reflected light image of column feed material collected from LPA. Bright phases are pyrite and magnetite and are visible in the four grains towards the top of the image, where they are mostly locked in a silicate matrix (diameter of grain mount, 3 cm).

The modal mineralogy as calculated by MLA-SEM confirmed magnesite, dolomite, quartz and chlorite as the dominate minerals with trace pyrite (Figure 5). Detailed investigations performed on pyrite showed that this sample has a *p80* of approximately 260 µm with the largest particle size reported as 355 µm (Figure 6). As large pyrite grains have a smaller surface area for oxidation, this means that the propensity for acid formation is theoretically further retarded than if populated with smaller grains (i.e., a *p80* of 50 µm). Examination of pyrite shows in general it has a euhedral-subhedral morphology across the observed grain size range (Figure 7). Pyrite mineral associations are dominantly with quartz (29 %), chlorite (27 %), magnesiohornblende (11 %) magnetite (5.5 %) with epidote (5 %) dominantly associated with smaller grains (Figures 7 and 8). Only three grains were –chalcopyrite associated, with no notable carbonate associations (Figures 7 and 8). In total, only 12 % of pyrite grains are liberated, suggesting, that based on these textural parameters too, a net alkaline condition is expected to persist in this column with a long-lag time to sulphide oxidation anticipated (Figure 8).

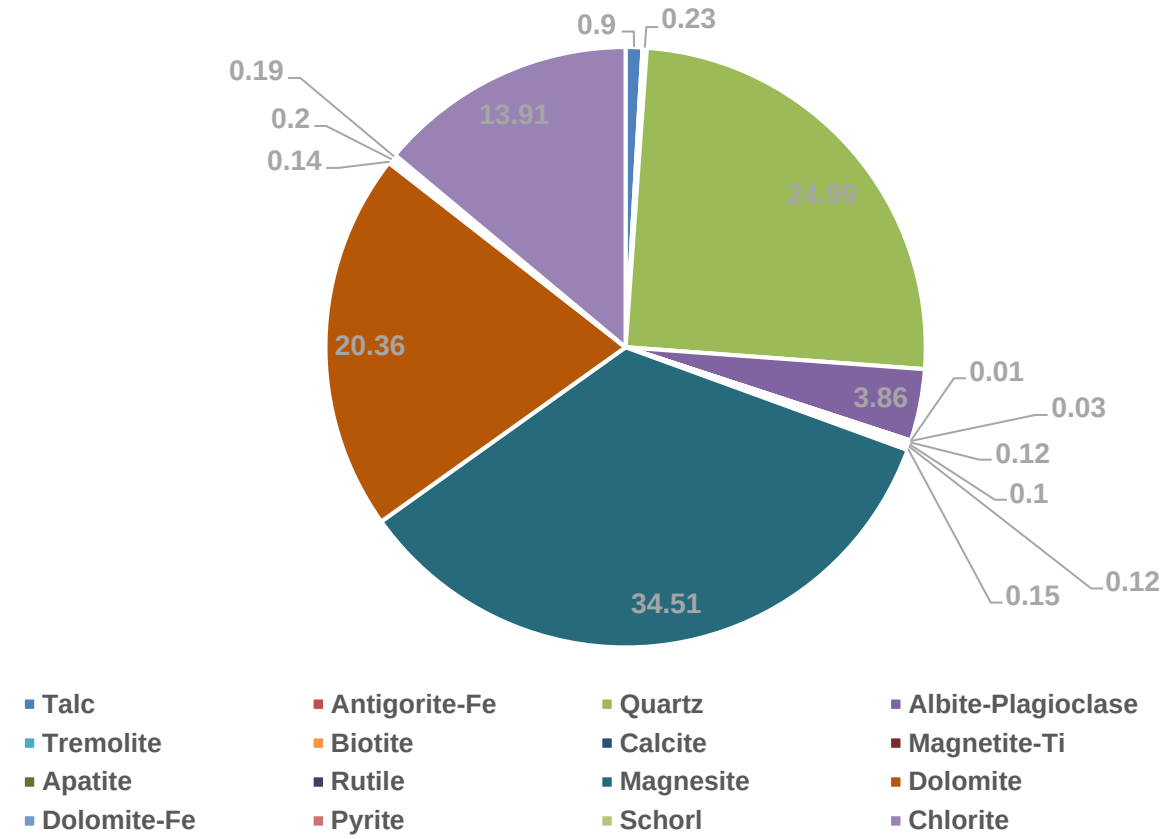

Figure 5. Modal mineralogy as calculated by MLA-SEM for LPA (week 0).

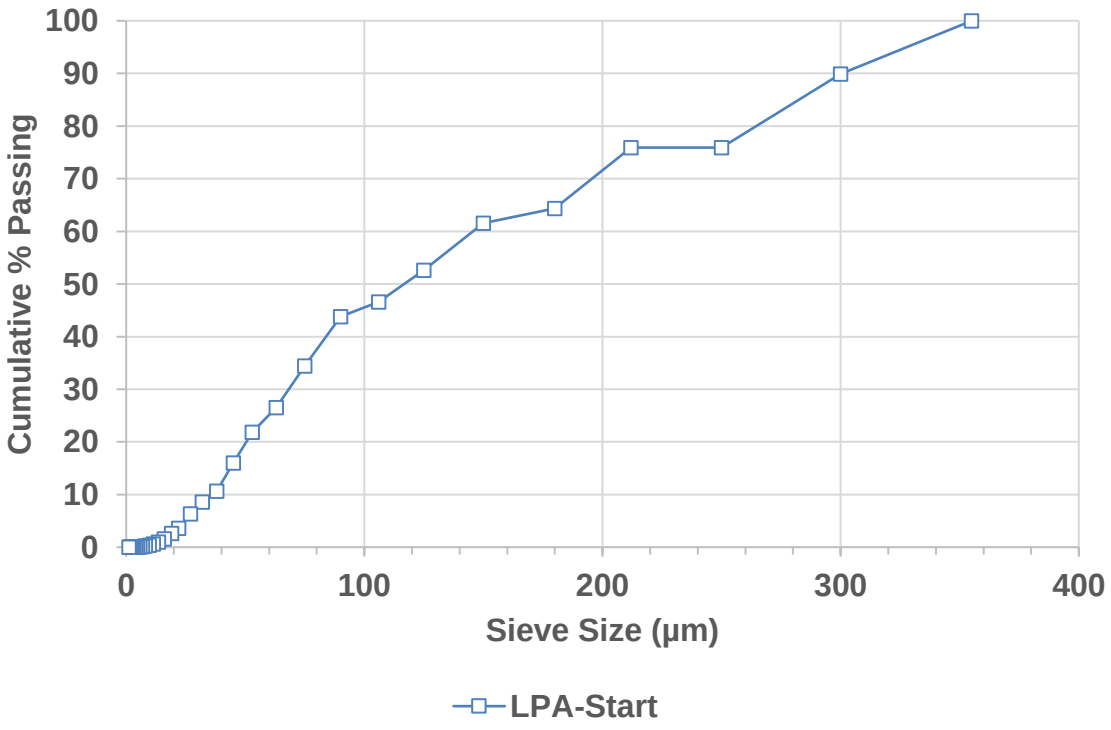

Figure 6. Pyrite grain size distribution (as calculated from MLA-SEM analysis).

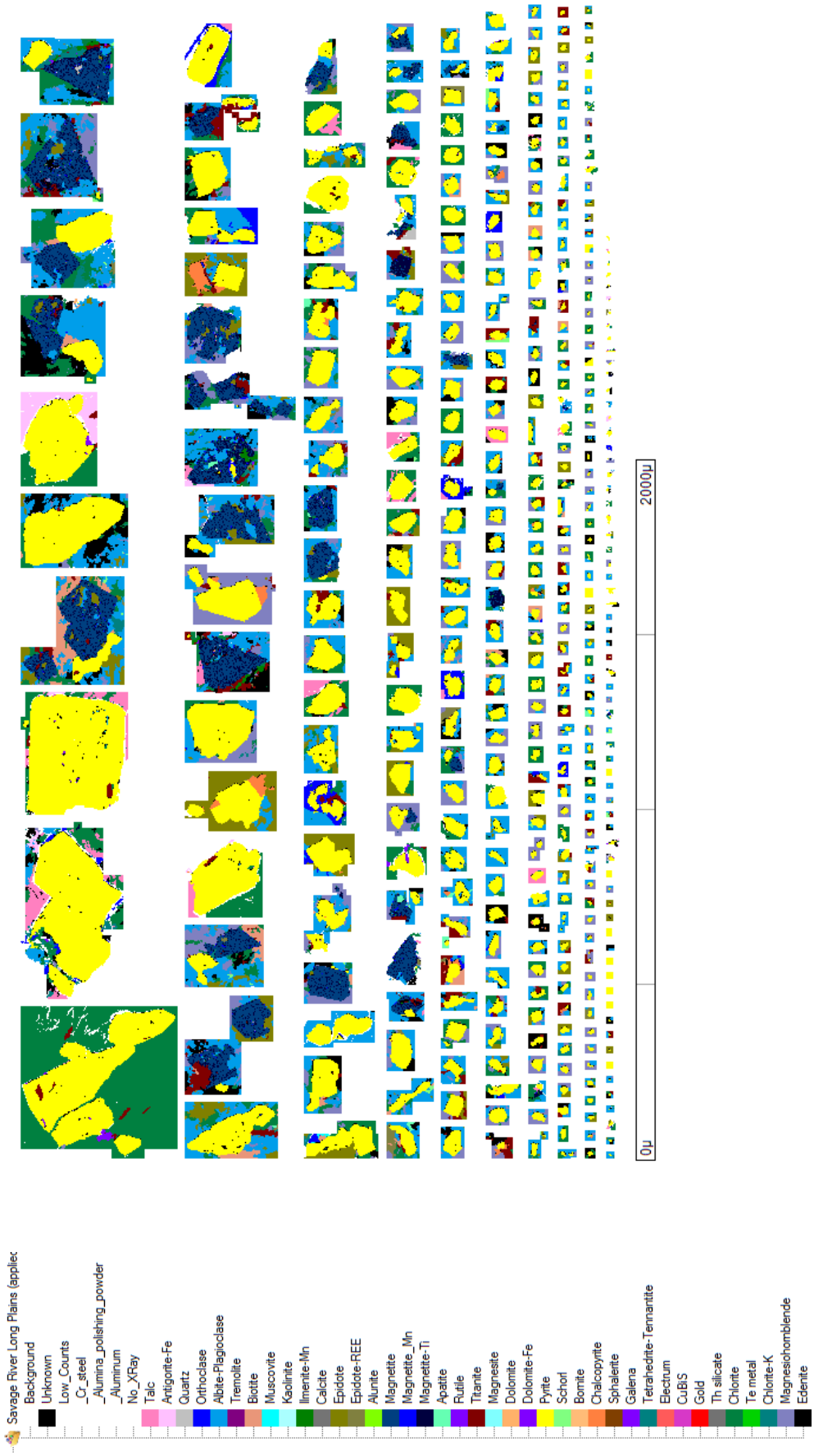

Figure 7. Classified pyrite grains in LPA with their mineral associations shown.

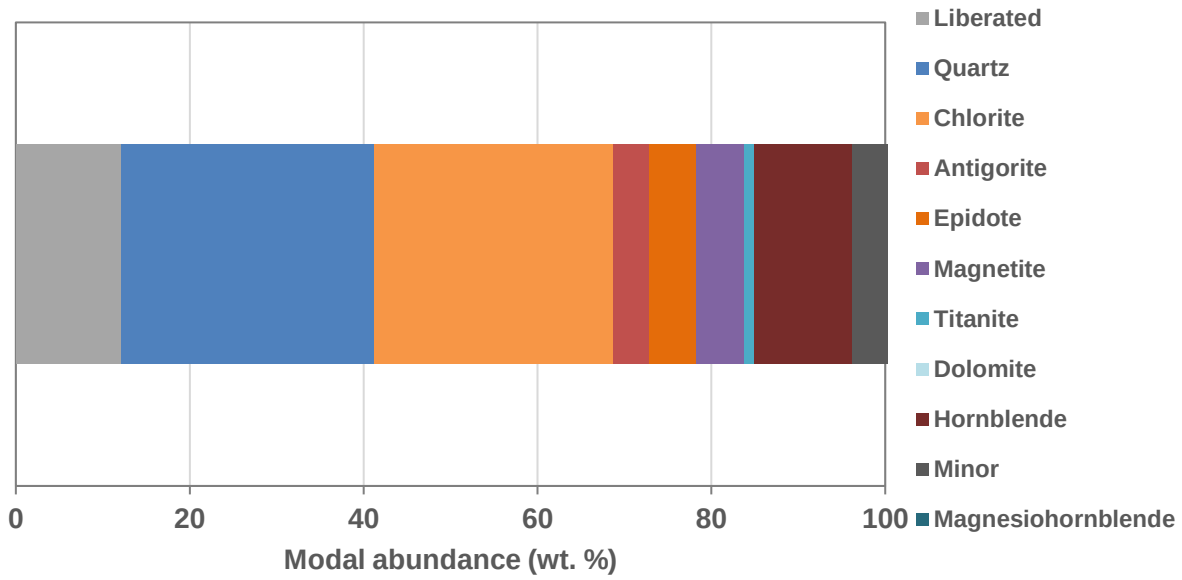

Figure 8. Pyrite locking and liberation of the column feed materials (week 0, calculated from MLA-SEM analysis).

Kinetic testing of Type A material confirmed it has remained as NAF (i.e., > pH 4.5) for the entirety of the three-year testing (Figure 9) with an average pH of 7.6. A notable decline in pH was noted around week 132-136 (pH 6.6-6.8) but this soon increased back to pH 7.6 where the pH remained within 0.4 pH units for the next 8 weeks before it once again began to decrease. The final pH measured was pH 7.1. MLA investigations confirm that 88% of minor pyrite is locked so the return of pH's in this range would be expected. The electrical conductivity was broadly low with a maximum value of 144.6 µs/cm^{-1} reported at week 90 and a range of 65 µs/cm^{-1} (Figure 9). One notable feature is that whilst this A-Type sample returned pH values much lower than expected for this waste. This conflicts with the notably high proportion of carbonates in the A Type waste encountered, as typically both dolomite and magnesite are expected to be reactive under these conditions (Noble et al., 2016). These results can be considered as positive from the perspective that alkaline mine drainage is not therefore considered a significant risk posed by these carbonate-rich materials. In the collected leachates the most consistently detected elements in leachates across this trial included Al (max: 0.86 mg/L; week 12), Cu (max: 0.02 mg/L; week 62), Mn (max: 0.006 mg/L; week 12) and Zn max: 0.089 mg/L; week 135; Table 5). Exceedances relative to the 80% ANZECC (2000) aquatic protection values were identified for Al and Cu (Table 5) with Al appearing to decrease over time (Figure 9) whilst Cu oscillates (relating to the liberation of trace pyrite as the experiment progressed) but relative to earlier weeks appears to now be declining, with its mass release rate dropping over time. Sulphate was measured in all leachates (<9 mg/L) except at week 131 and for all week's values are far below the WHO (2006) DWG value (400 mg/L; no ANZECC (2000) aquatic protection value was located). The continued detection of sulphate suggests protracted oxidation of trace pyrite with automated mineralogy results confirming that this should be expected (Figure 7) again due to weathering and liberation of pyrite, particularly those bound by chlorite and epidote (Figure 8; in accordance with Sverdrup, 1990). Low concentrations (i.e., lower than expected) of Ca and Mg (< 6 mg/L) were measured in the leachate (Table 5) suggesting that magnesite and dolomite are weathering very slowly in these conditions which is consistent with the final bulk mineralogy (62.5 % remains; Figure 11) and pH measurements. Collectively the results suggest that A-Type is a very effective neutralising material.

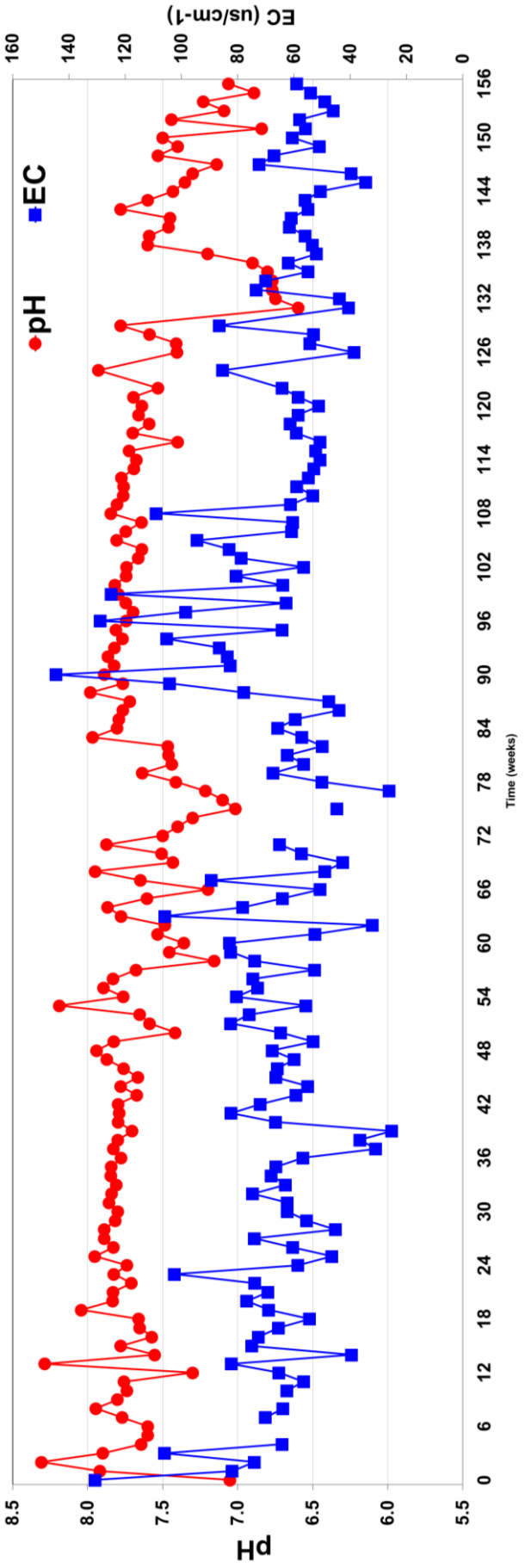

Figure 9. Measurement of pH and EC values for Type A waste material (weeks 0 to 156).

Table 5. Chemistry of Type A waste leachates, measured from week 0 to week 155 (all data in mg/l).

WEEK	SO_4	Al	Be	Ba	Co	Cu	Pb	Mn	Zn	B	Ca	Mg
ANZECC (2000) 80% protection	-	*0.15*	*N/D*	*N/D*	*N/A*	*0.0025*	*0.0094*	*3.6*	*0.031*	*1.3*	*N/D*	*N/D*
0	9	0.005	0.002	0.0005	0.001	0.0005	0.0005	0.0005	0.0025	0.025	ND	ND
4	4	0.04	0.0005	0.002	0.0005	0.002	0.0005	0.001	0.0025	0.25	ND	ND
8	4	0.2	0.0005	0.001	0.0005	0.01	0.0005	0.004	0.0025	0.025	ND	ND
12	8	0.86	0.0005	0.001	0.0005	0.021	0.001	0.006	0.0025	0.025	ND	ND
16	5	0.25	0.0005	0.0005	0.0005	0.007	0.0005	0.002	0.0025	0.025	ND	ND
20	3	0.48	0.0005	0.001	0.0005	0.01	0.0005	0.002	0.0025	0.025	ND	ND
24	3	0.3	0.0005	0.0005	0.0005	0.007	0.0005	0.001	0.0025	0.025	ND	ND
30	5	0.005	0.002	0.0005	0.009	0.0005	0.0005	0.001	0.0025	0.025	ND	ND
34	7	0.11	0.0005	0.0005	0.0005	0.01	0.0005	0.0005	0.0025	0.025	ND	ND
38	4	0.29	0.0005	0.002	0.0005	0.006	0.0005	0.001	0.006	0.025	ND	ND
42	4	0.12	0.0005	0.001	0.0005	0.022	0.0005	0.002	0.0025	0.14	ND	ND
46	4	0.14	0.0005	0.0005	0.0005	0.002	0.0005	0.002	0.0025	0.025	ND	ND
50	3	0.09	0.0005	0.0005	0.0005	0.002	0.0005	0.001	0.0025	0.025	ND	ND
54	6	0.08	0.0005	0.002	0.0005	0.009	0.0005	0.002	0.0025	0.025	2	3
58	4	0.13	0.0005	0.001	0.0005	0.012	0.0005	0.0005	0.0025	0.025	2	3
62	1	0.15	0.0005	0.001	0.0005	0.021	0.0005	0.003	0.0025	0.025	3	4
66	4	0.08	0.0005	0.0005	0.0005	0.0005	0.0005	0.002	0.0025	0.025	1	2
70	4	0.12	0.0005	0.001	0.0005	0.006	0.0005	0.002	0.0025	0.025	1	2
75	0.5	0.16	0.0005	0.002	0.0005	0.01	0.0005	0.003	0.0025	0.025	1	2
78	4	0.11	0.0005	0.001	0.0005	0.003	0.0005	0.002	0.0025	0.025	1	2
82	3	0.03	0.0005	0.153	0.0005	0.005	0.0005	0.001	0.051	0.06	4	6
86	3	0.04	0.0005	0.158	0.0005	0.007	0.0005	0.0005	0.050	0.06	3	4
90	4	0.03	0.0005	0.220	0.0005	0.003	0.0005	0.001	0.046	0.10	4	5
94	3	0.07	0.0005	0.122	0.0005	0.007	0.0005	0.0005	0.050	0.05	3	4
98	3	0.04	0.0005	0.136	0.0005	0.005	0.0005	0.0005	0.058	0.025	3	5
102	4	0.07	0.0005	0.142	0.0005	0.005	0.0005	0.001	0.051	0.025	3	4
106	3	0.06	<0.001	0.002	<0.001	0.003	<0.001	<0.001	<0.005	<0.05	2	3
110	2	0.07	<0.001	0.002	<0.001	0.004	<0.001	<0.001	<0.005	<0.05	1	2
114	2	0.12	<0.001	0.002	<0.001	0.002	<0.001	0.002	<0.005	<0.05	1	2
118	2	0.09	<0.001	0.002	<0.001	0.002	<0.001	0.001	0.009	<0.05	1	3
122	2	0.05	<0.001	0.002	<0.001	0.001	<0.001	0.001	<0.005	<0.05	1	3
126	3	0.08	<0.001	0.002	<0.001	0.001	<0.001	0.001	<0.005	<0.05	<1	2
131	<1	0.07	<0.001	0.002	<0.001	0.006	<0.001	0.002	<0.005	<0.05	<1	2
135	4	0.09	ND	ND	<0.001	0.005	<0.001	0.002	0.089	ND	3	5
139	3	0.12	ND	ND	<0.001	0.005	<0.001	<0.001	<0.005	ND	3	4
143	1	0.05	ND	ND	<0.001	0.007	<0.001	0.001	0.009	ND	3	6
147	1	0.05	ND	ND	<0.001	0.009	<0.001	0.002	<0.005	ND	1	2
151	2	0.06	ND	ND	<0.001	0.012	<0.001	0.003	0.057	ND	3	5
155	1	0.03	ND	ND	<0.001	0.005	<0.001	<0.001	0.085	ND	3	5

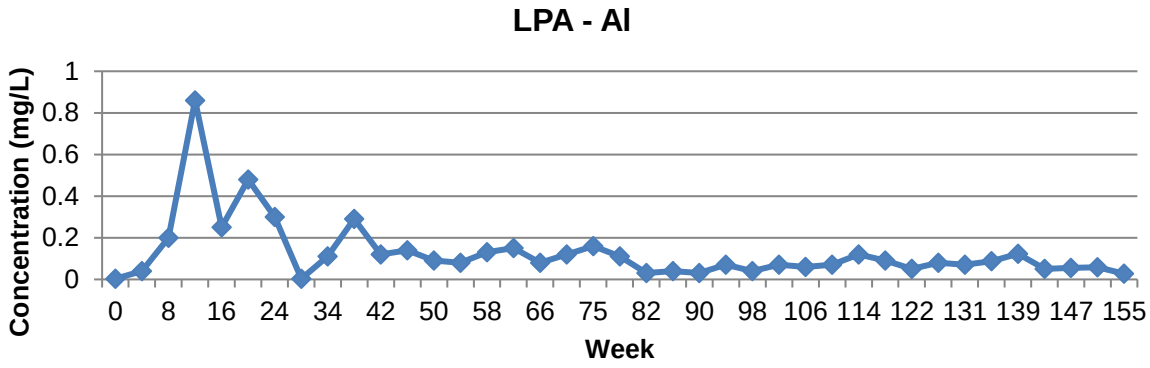
LPA - Al
Concentration (mg/L)
1
0.8
0.6
0.4
0.2
0
0 8 16 24 34 42 50 58 66 75 82 90 98 106 114 122 131 139 147 155
Week

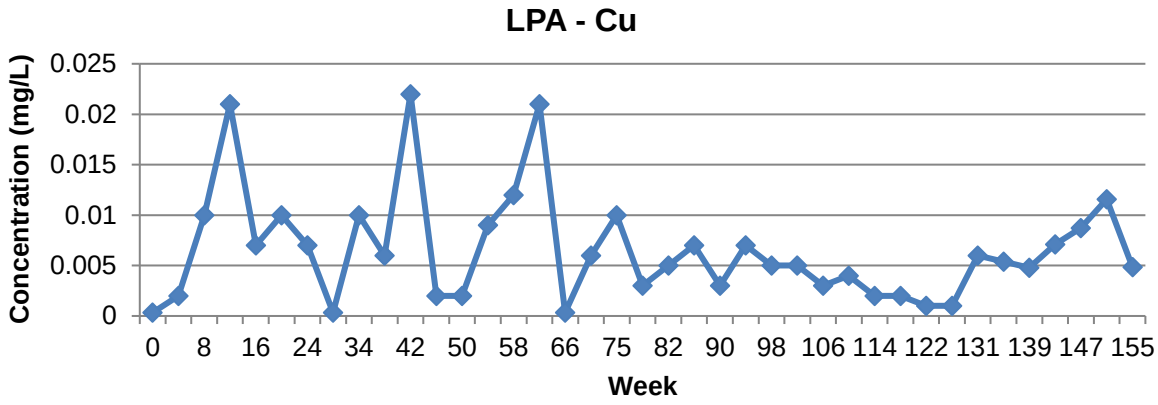
LPA - Cu
Concentration (mg/L)
0.025
0.02
0.015
0.01
0.005
0
0 8 16 24 34 42 50 58 66 75 82 90 98 106 114 122 131 139 147 155
Week

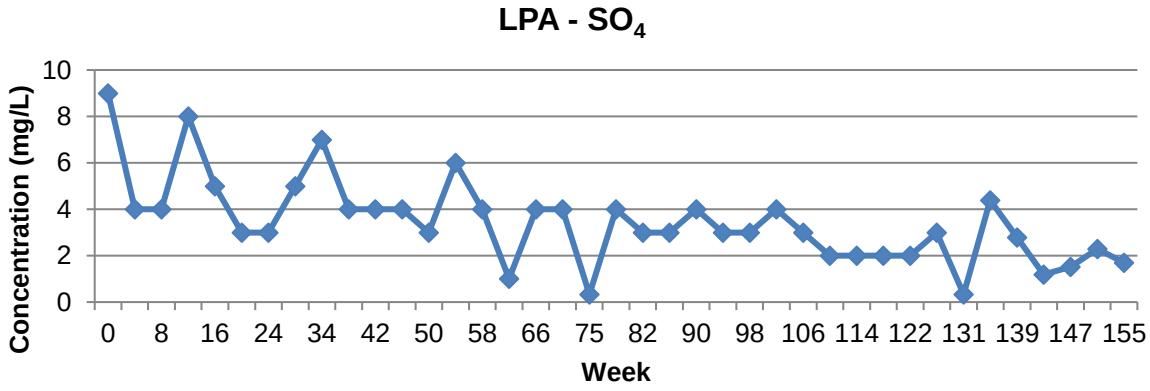
LPA - SO4
Concentration (mg/L)
10
8
6
4
2
0
0 8 16 24 34 42 50 58 66 75 82 90 98 106 114 122 131 139 147 155
Week

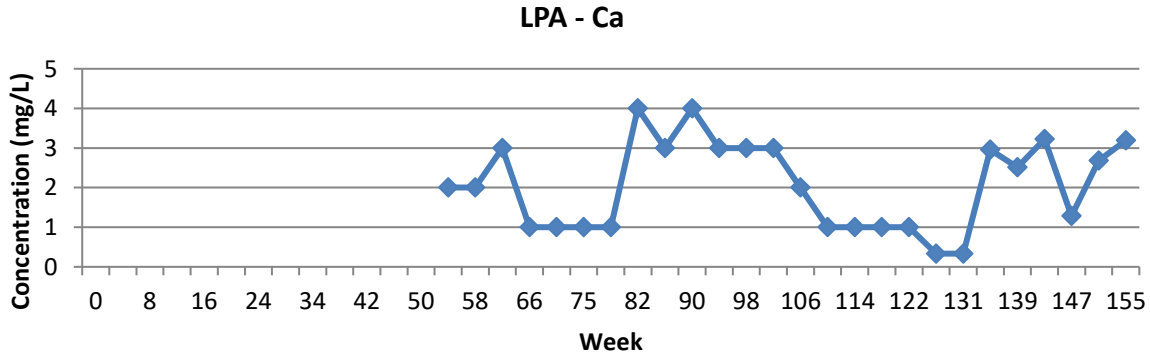
LPA - Ca
Concentration (mg/L)
5
4
3
2
1
0
0 8 16 24 34 42 50 58 66 75 82 90 98 106 114 122 131 139 147 155
Week

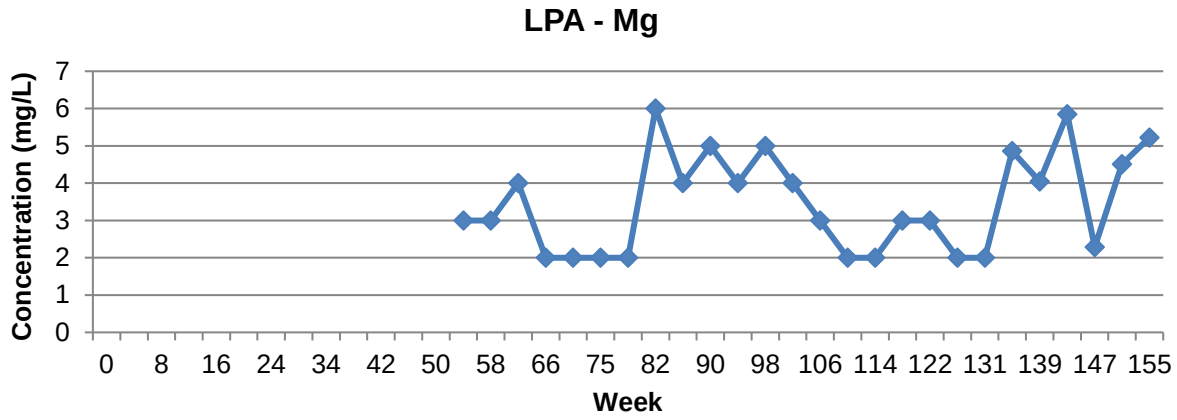

Figure 10. Measurement of Al, Cu, SO_4, Ca and Mg for Type A leachates.

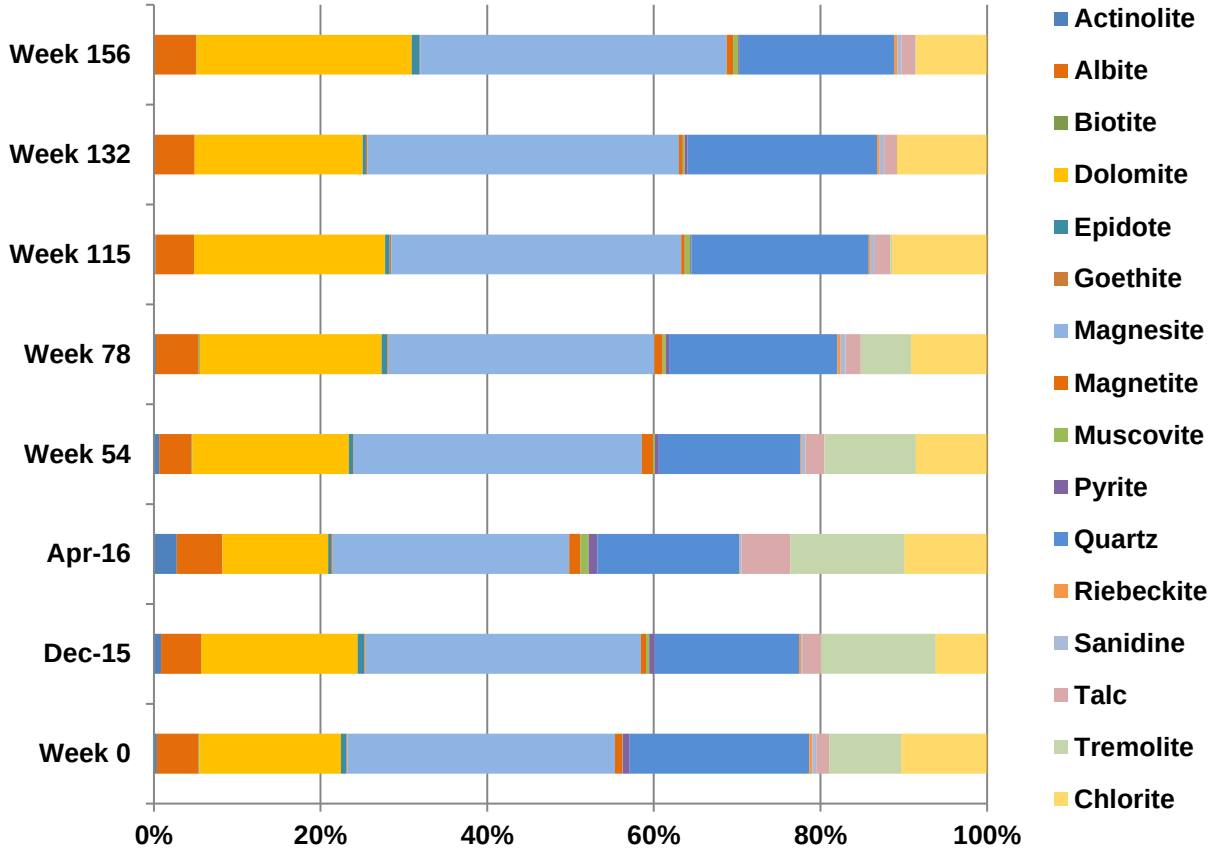

Figure 11. Bulk mineralogy of Type A waste material (measured by XRD).

3.2 Waste Type B

The column feed bulk mineralogy (i.e., week 0) of B-Type (measured by XRD) is dominated by albite (35 wt. %), tremolite (18 wt. %), actinolite (15 wt. %) and chlorite (11 wt. %) with minor pyrite (1.15 wt.%)and trace magnetite (< 1 wt. %). Carbonates are present in trace concentrations only (< 1 % dolomite and magnesite). Reflected light images demonstrate that, pyrite is coarser and more disseminated than in A-Type but is locked-up in actinolite and tremolite or semi-liberated (i.e., proximal to particle boundaries; Figure 12). Based on these observations, the net pH recorded from

this kinetic trial would be lower than that for A-Type, and given the neutraliser absence, circum-neutral to weakly acidic leachates would be expected for the duration of the trial.

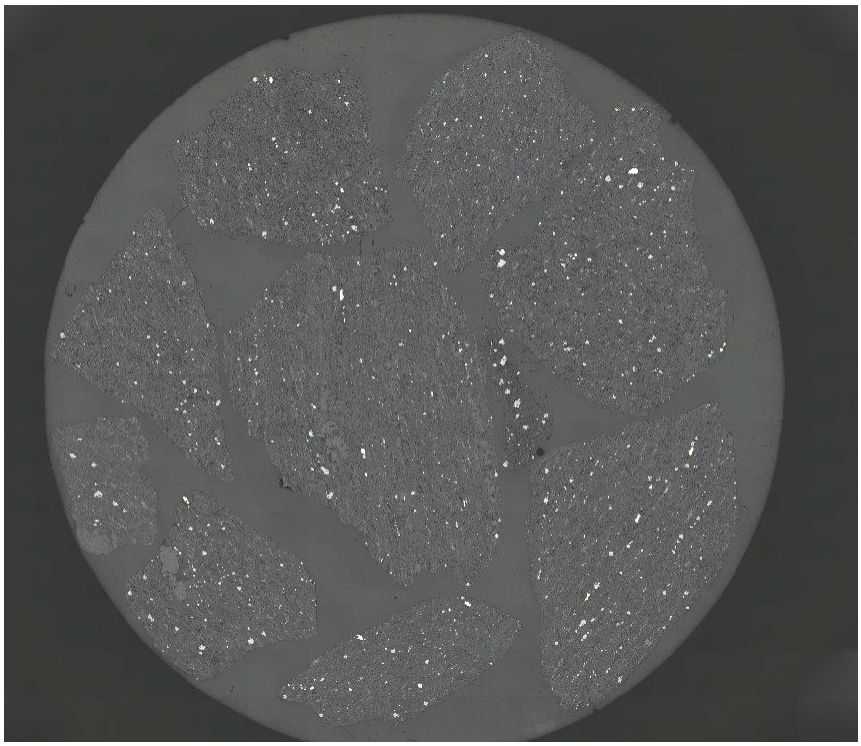

Figure 12. Reflected light image of column feed material collected from LPB. Bright phases are pyrite and magnetite and are visible in the four grains towards the top of the image, where they appear mostly locked in a tremolite/actinolite matrix (diameter of grain mount, 3 cm).

The modal mineralogy as calculated by MLA-SEM was consistent with bulk mineralogy (XRD) measurements and reported feldspar (albite; 31 %), magnesiohornblende (19%) and chlorite (12%) as dominating. Edenite (12%) was identified by MLA and is an amphibole which has been identified in this type of mineral deposit setting (i.e., metamorphic, occurring in pods within a carbonate formation; Figure 13). Detailed investigations performed on pyrite showed that this sample has similar properties to the A-Type sample with a *p80* of approximately 250 µm and the largest particle size also reported as 355 µm (Figure 14). These results suggest that the leachate collected during the experiment may return pH values higher than expected than if predictions were based solely on the bulk mineralogy (which would suggest the sample is PAF when considering the pyrite to carbonate balance). Classified mineralogy images of pyrite and its associated minerals shows it is present dominantly as euhedral-subhedral grain across the observed size range (Figure 15). Larger grains appear dominated by antigorite, whilst smaller grains are associated with feldspar (Figure 15). Calculated pyrite mineral associations show that 12.5 % are liberated (Figure 16). Detailed analyses confirmed that larger grains are dominantly feldspar-associated (27.5 %), chlorite (20 %), antigorite (8.5 %) and hornblende (11 %) with magnetite (5.6 %) and epidote (5 %) dominantly associated with smaller grains (Figures 15 and 16). Only a few grains (< 10) were –chalcopyrite associated, with no notable carbonate associations (Figures 15 and 16). These results also suggest that based on textural parameters a net alkaline condition would be expected to persist in this column as pyrite appears encapsulated (with minor periodic drops in pH expected as pyrite is liberated- i.e., < 0.5 pH units). However, when pyrite does undergo oxidation, as it is chalcopyrite-associated, Cu would be expected to leach.

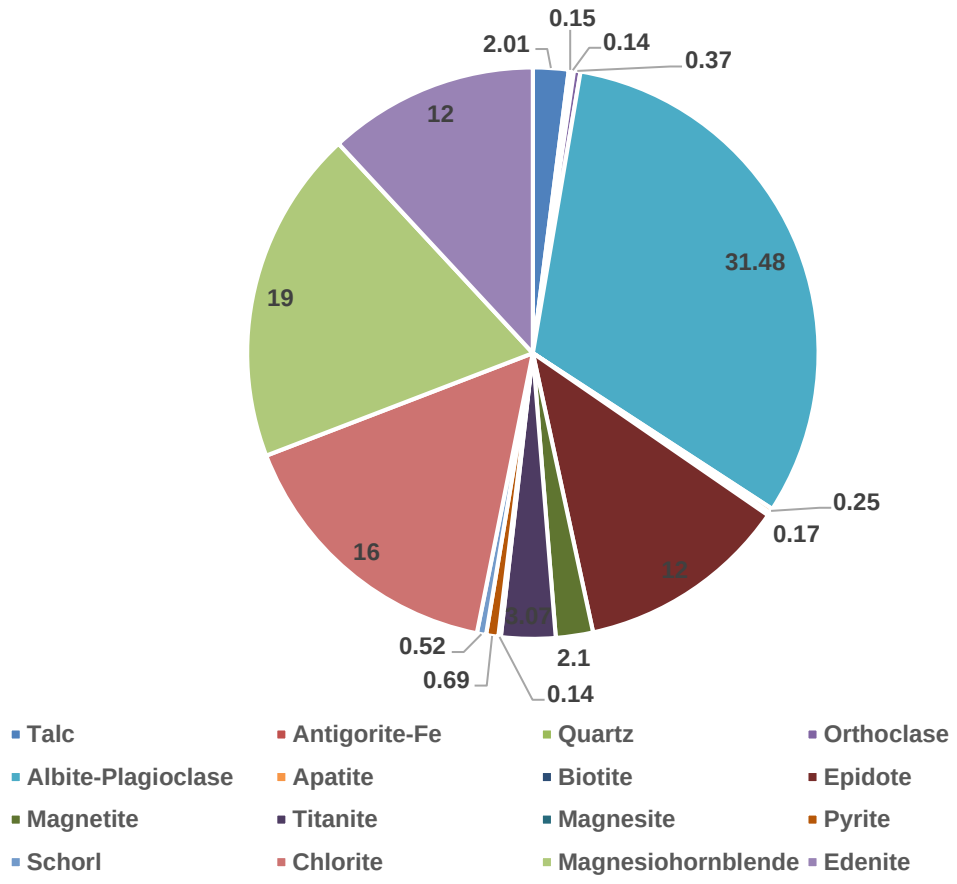

Figure 13. Modal mineralogy as calculated by MLA-SEM for LPB (week 0).

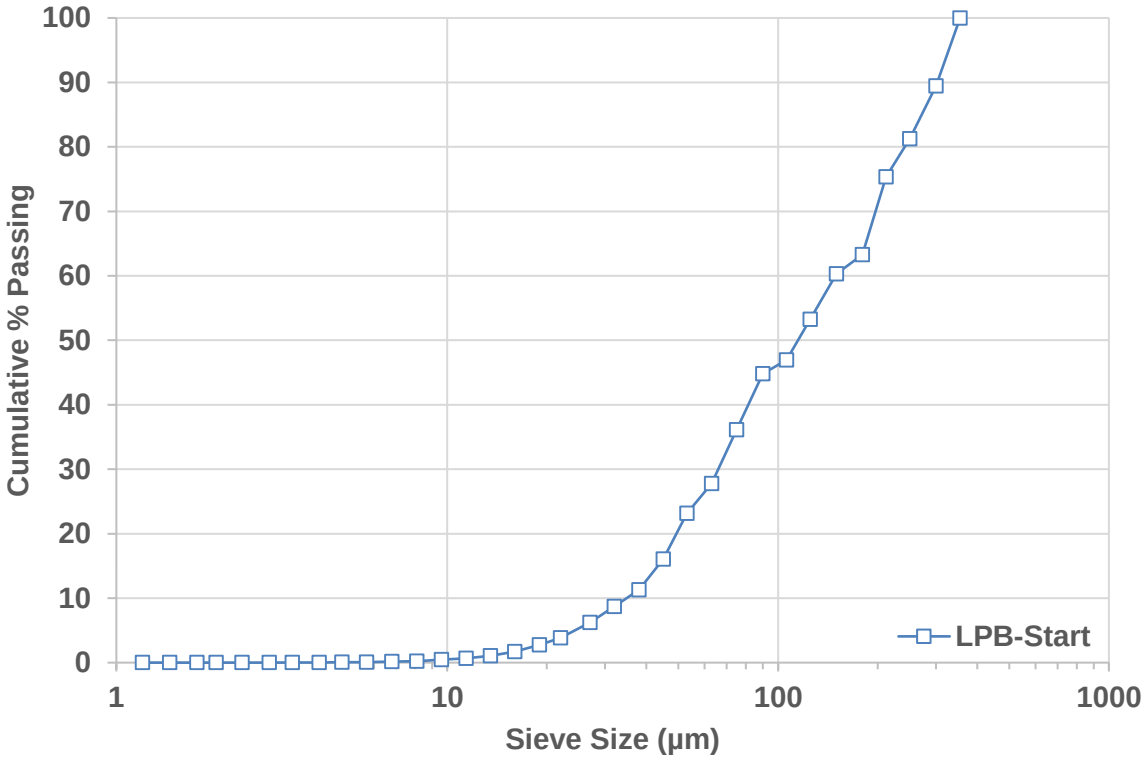

Figure 14. Pyrite grain size distribution (as calculated from MLA-SEM analysis).

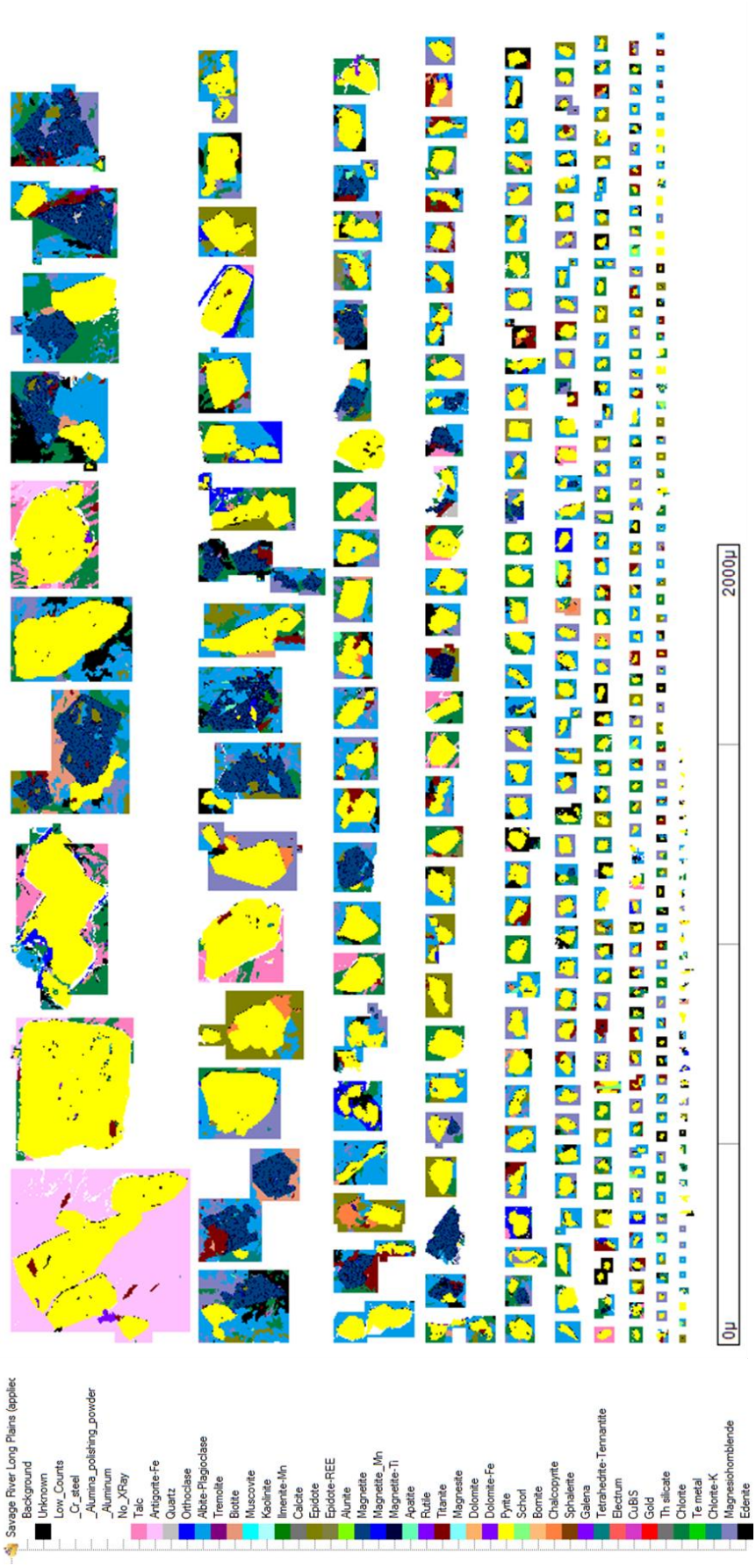

Figure 15. Classified pyrite grains in LPB with their mineral associations shown.

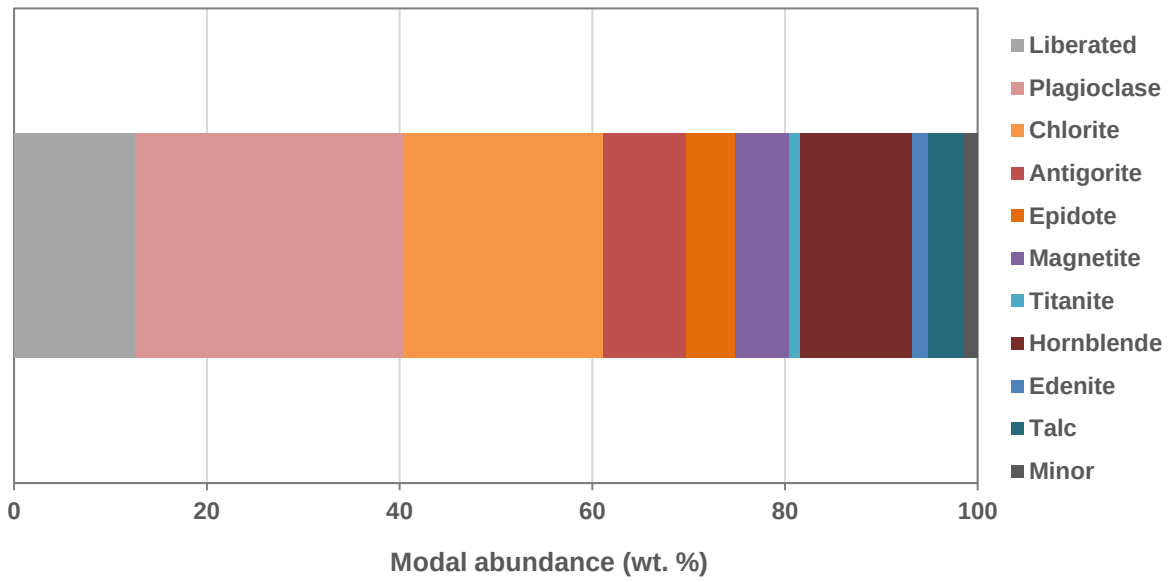

Figure 16. Pyrite locking and liberation of the column B feed materials (week 0, calculated from MLA-SEM analysis).

Kinetic testing of Type B material also confirmed it as NAF (pH > 4.5) for the entire duration of the experiment (Figure 17). The electrical conductivity measurements were considered moderate over this experiment (range: 45 to 625 µs/cm^{-1}) with this maximum reported at week 29. In general, an average of 180 µs/cm^{-1} was calculated. Much like Type A, the pH appeared to have stabilised from week 87 to 112, but after this time it oscillated from weeks 121 to 129 (from pH 7.1 to 7.6) and at weeks 130 and 131 it once again dropped to pH 6.6 and 6.4. From week 138 it increased to pH 7.6 but then began to gradually decline for the remained of the trial to a final pH of 7.1. These results are supported by the MLA observations made and show that in the first few weeks, it is likely that partially liberated pyrite had oxidised with a passivating coating formed therefore sealing it off from further oxidation (and any potential fines in the column feed material are rapidly reacting). For the majority the trial, pyrite is encapsulated but the grains associated with chlorite and antigorite are periodically liberated/partially liberated causing the pH drops that are observed at weeks 66 and 132. These are likely to also form protective iron-oxide surface coating sealing them off from further oxidation, hence the pH recoveries, but as the reactive minerals (Sverdrup, 1990) continue to weather different parts of these grains become exposed and then once again, coatings form. Overall, this column had an average pH of 7.4. Sulphate data is correspondingly higher in the collection weeks 126, 131 and 135 58 to 147 mg/L (Table 6) where pH values were at their lowest (except for at the start of the experiment). Overall, sulphate values are much higher than Type A, showing this contains more (reactive) pyrite as bulk mineralogy results suggest. Sulphate concentrations appear to be decreasing towards the end of the trial (Figure 18). Leachate data for Ca and Mg show greater elution in comparison to Type A, particularly in the last six months of measurements (weeks 131; max. of 36 and 16 mg/L measured respectively; Table 6) but likely corresponds to dissolution of transient sulphates (gypsum was observed to form on the surface when the heating lamps were on) or silicates and not a reflection of neutralisation. Relative to the ANZECC (2000) aquatic protection 80% protection values, Cu is consistently elevated (maximum: 0.02 mg/L; week 8) with Al also high but appearing to decline in the last six-month period (Table 6; Figure 18). The final Zn (0.02 mg/L) measurement also exceeded the ANZECC (2000) 80% guideline but it is suspected this is erroneous as the control reports Zn.

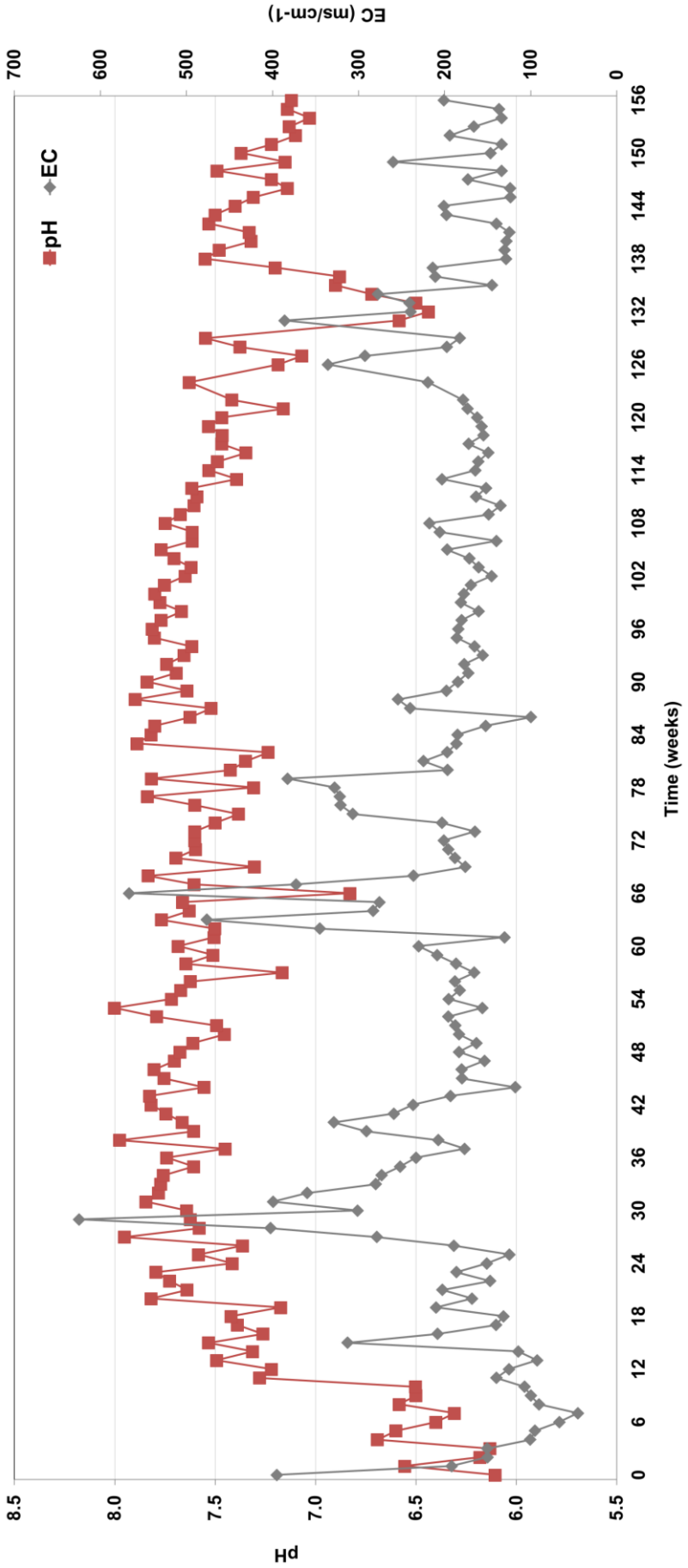

Figure 17. Measurements of pH and EC for Type B waste material (week 0 to 156).

Table 6. Chemistry of Type B waste leachates, measured from week 0 to week 155 (all data in mg/L).

WEEK	SO_4	Al	As	Be	Ba	Co	Cu	Pb	Mn	V	Zn	Ca	Mg
ANZECC (2000) 80% protection		*0.15*	*0.14*	*N/D*	*N/D*	*N/A*	*0.0025*	*0.0094*	*3.6*	*N/D*	*0.031*	N/D	N/D
0	39	0.005	0.0005	0.004	0.0005	0.002	0.0005	0.028	0.004	0.006	0.0025	ND	ND
4	10	0.03	0.0005	0.0005	0.002	0.0005	0.002	0.0005	0.002	0.005	0.0025	ND	ND
8	80	0.05	0.0005	0.0005	0.004	0.0005	0.02	0.0005	0.01	0.005	0.0025	ND	ND
12	82	0.06	0.0005	0.0005	0.004	0.0005	0.011	0.002	0.008	0.005	0.0025	ND	ND
16	68	0.1	0.0005	0.0005	0.004	0.0005	0.014	0.0005	0.003	0.005	0.0025	ND	ND
20	60	0.2	0.0005	0.0005	0.004	0.0005	0.01	0.0005	0.004	0.005	0.0025	ND	ND
24	161	0.15	0.0005	0.0005	0.01	0.0005	0.01	0.0005	0.006	0.005	0.0025	ND	ND
30	158	0.005	0.0005	0.009	0.0005	0.011	0.0005	0.003	0.0005	0.005	0.07	ND	ND
34	230	0.11	0.0005	0.0005	0.012	0.0005	0.015	0.0005	0.004	0.005	0.0025	ND	ND
38	59	0.31	0.0005	0.0005	0.006	0.0005	0.005	0.0005	0.0005	0.005	0.006	ND	ND
42	74	0.06	0.0005	0.0005	0.004	0.0005	0.014	0.0005	0.001	0.005	0.0025	ND	ND
46	55	0.13	0.0005	0.0005	0.004	0.0005	0.006	0.0005	0.004	0.005	0.006	ND	ND
50	51	0.08	0.0005	0.0005	0.003	0.0005	0.004	0.0005	0.0005	0.005	0.0025	ND	ND
54	70	0.07	0.0005	0.0005	0.005	0.0005	0.009	0.0005	0.0005	0.005	0.0025	14	8
58	69	0.1	0.0005	0.0005	0.004	0.0005	0.009	0.0005	0.0005	0.005	0.0025	14	8
62	162	0.07	0.0005	0.0005	0.009	0.0005	0.016	0.0005	0.006	0.005	0.0025	31	17
66	290	0.05	0.003	0.0005	0.016	0.0005	0.004	0.001	0.053	0.005	0.015	56	33
70	64	0.09	0.0005	0.0005	0.005	0.0005	0.012	0.0005	0.002	0.005	0.0025	14	8
75	142	0.21	0.0005	0.0005	0.011	0.0005	0.017	0.0005	0.003	0.005	0.008	28	13
78	153	0.1	0.0005	0.0005	0.012	0.0005	0.006	0.0005	0.022	0.005	0.006	32	14
82	65	0.03	0.0005	0.0005	0.119	0.0005	0.008	0.0005	0.001	0.005	0.054	20	9
86	63	0.11	0.0005	0.0005	0.125	0.0005	0.005	0.0005	0.0005	0.005	0.066	18	7
90	59	0.04	0.0005	0.0005	0.106	0.0005	0.005	0.0005	0.0005	0.005	0.059	18	8
94	48	0.05	0.0005	0.0005	0.079	0.0005	0.006	0.0005	0.001	0.005	0.062	15	6
98	50	0.04	0.0005	0.0005	0.096	0.0005	0.008	0.0005	0.0005	0.005	0.054	15	6
102	46	0.04	0.0005	0.0005	0.093	0.0005	0.005	0.0005	0.001	0.005	0.056	14	6
106	40	0.05	<0.001	<0.001	0.004	<0.001	0.003	<0.001	<0.001	<0.01	<0.005	10	5
110	38	0.04	<0.001	<0.001	0.004	<0.001	0.003	<0.001	0.001	<0.01	<0.005	10	5
114	54	0.05	<0.001	<0.001	0.004	<0.001	0.002	<0.001	0.002	<0.01	<0.005	12	6
118	45	0.05	<0.001	<0.001	0.004	<0.001	0.002	<0.001	0.001	<0.01	0.006	11	5
122	58	0.05	<0.001	<0.001	0.004	<0.001	0.002	<0.001	0.001	<0.01	0.008	14	7
126	147	0.05	<0.001	<0.001	0.012	<0.001	0.002	<0.001	0.001	<0.01	<0.005	29	15
131	144	0.06	<0.001	<0.001	0.011	<0.001	0.004	<0.001	0.003	<0.01	<0.005	36	16
135	98	0.06	<0.001	ND	ND	<0.001	0.005	<0.001	0.002	<0.01	0.09	25	9
139	38	0.10	<0.001	ND	ND	<0.001	0.005	<0.001	0.001	<0.01	<0.005	13	5
143	39	0.06	<0.001	ND	ND	<0.001	0.007	<0.001	0.001	<0.01	0.01	15	6
147	68	0.08	<0.001	ND	ND	<0.001	0.008	<0.001	0.002	<0.01	<0.005	17	7
151	57	0.05	<0.001	ND	ND	<0.001	0.016	<0.001	0.013	<0.01	0.01	16	7
155	55	0.02	<0.001	ND	ND	<0.001	0.005	<0.001	0.001	<0.01	0.09	16	6

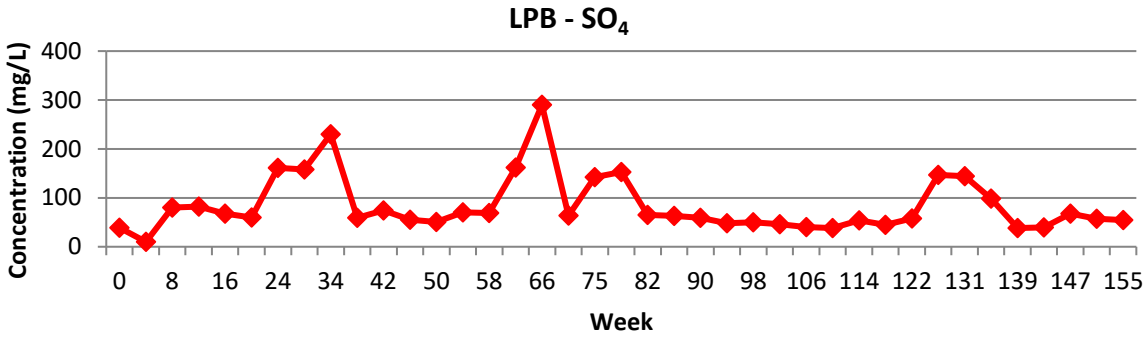
LPB - SO4
Concentration (mg/L)
400
300
200
100
0
0 8 16 24 34 42 50 58 66 75 82 90 98 106 114 122 131 139 147 155
Week

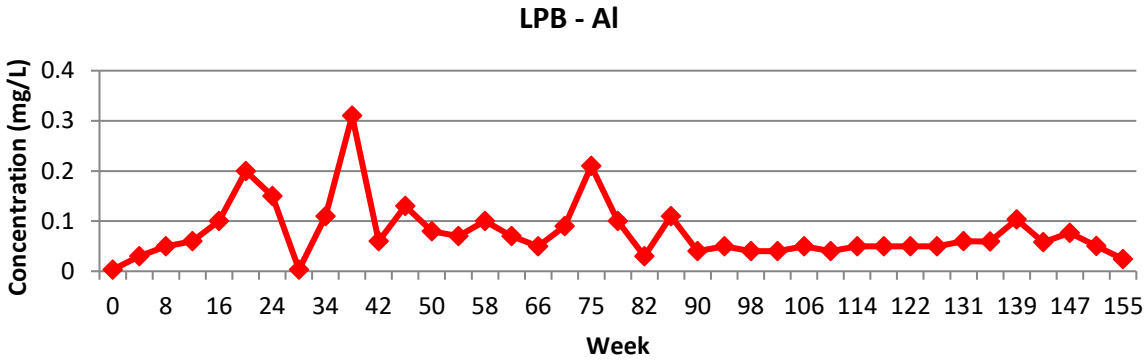
LPB - Al
Concentration (mg/L)
0.4
0.3
0.2
0.1
0
0 8 16 24 34 42 50 58 66 75 82 90 98 106 114 122 131 139 147 155
Week

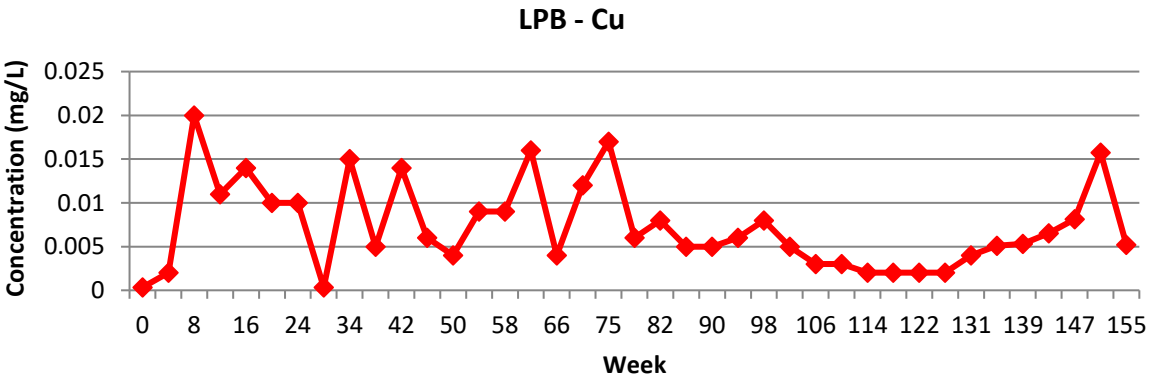
LPB - Cu
Concentration (mg/L)
0.025
0.02
0.015
0.01
0.005
0
0 8 16 24 34 42 50 58 66 75 82 90 98 106 114 122 131 139 147 155
Week

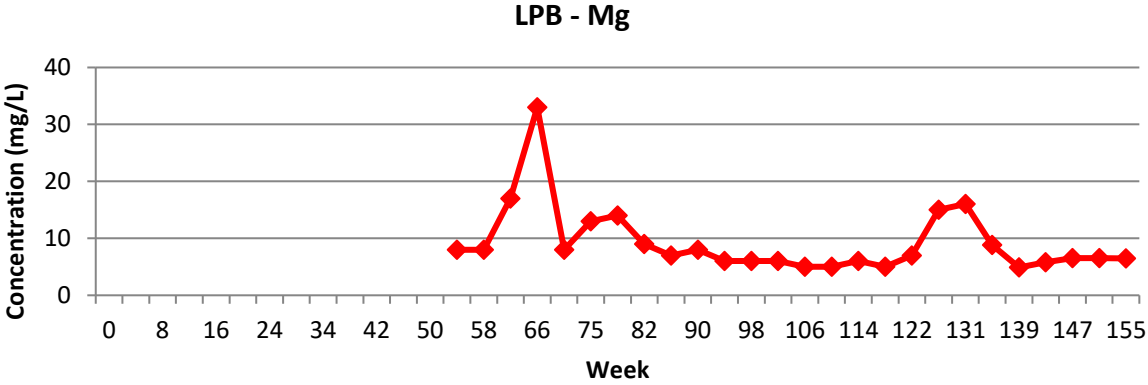
LPB - Mg
Concentration (mg/L)
40
30
20
10
0
0 8 16 24 34 42 50 58 66 75 82 90 98 106 114 122 131 139 147 155
Week

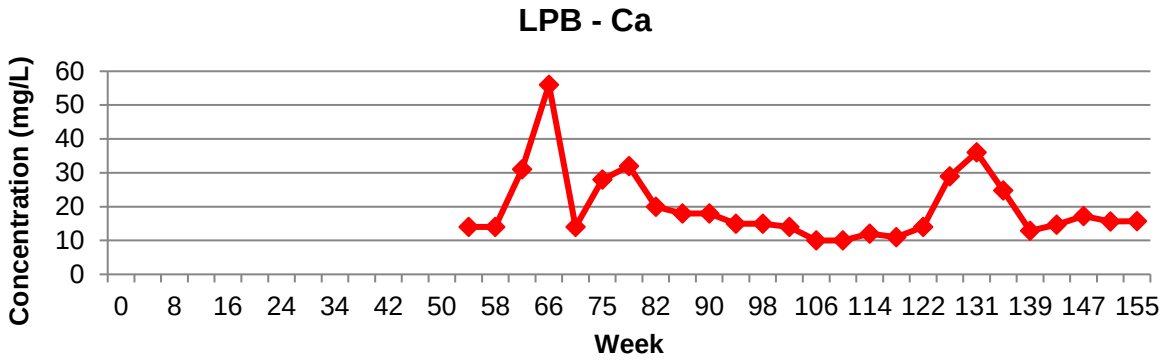

Figure 18. Measurement of Al, Cu, SO_4, Ca and Mg for Type B leachates.

The bulk mineralogy throughout the experiment shows that perhaps a greater reservoir of carbonates may exist than initially expected with minor magnesite (1 wt.%) measured at week 132, but doomite was consistently trace (Figure 19). In general, pyrite content decreased from 1.1 wt.% at week 0 to 0.7 wt. % at week 156, supporting all geochemical observations made for this column, but as it is such a minor phase, the reaction products (i.e., rims) cannot be identified by this technique (SEM analyses would be required) although trace goethite had been consistently reported (Figure 19). Overall, this column is considered NAF, though similar cyclicity of pH drops correlating with pyrite exposure are expected, though this will not push this sample into the PAF field. This waste type should not be considered an effective neutraliser, but could be blended with Type A.

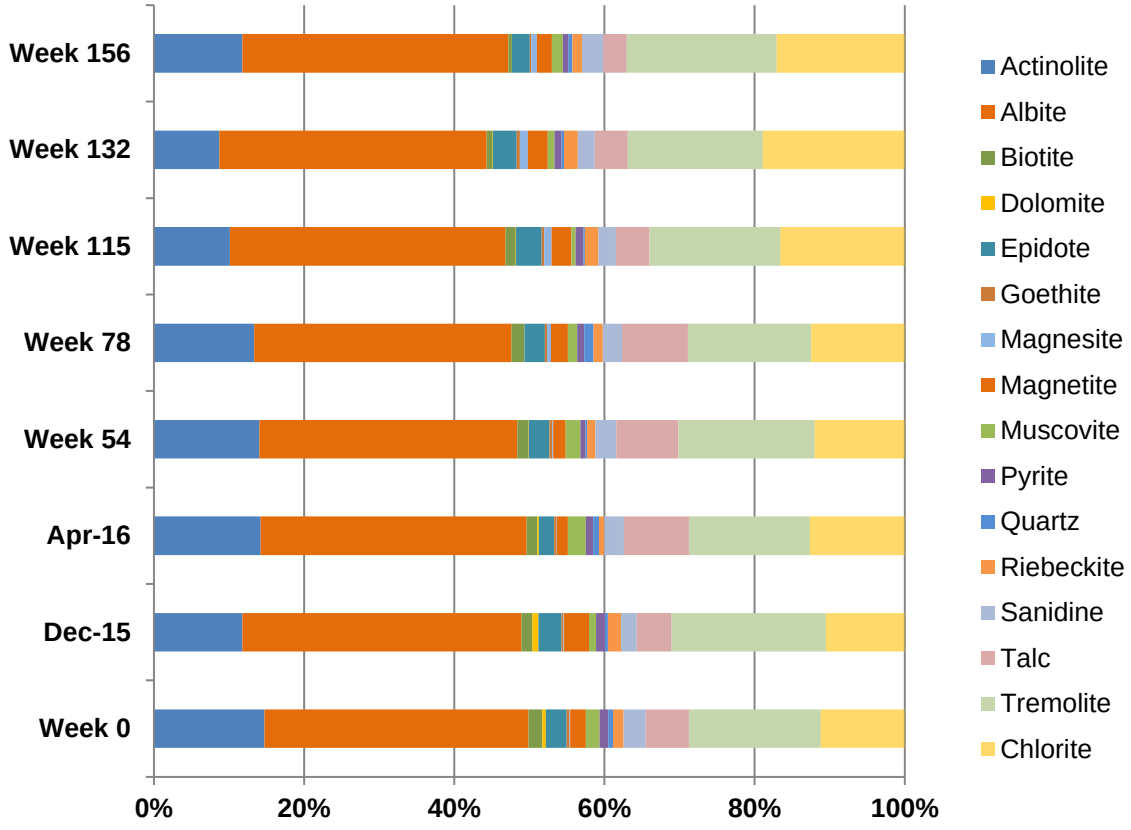

Figure 19. Bulk mineralogy of Type B waste material (measured by XRD).

3.3 Waste Type D

The column feed bulk mineralogy (i.e., week 0) of D-Type (measured by XRD) is dominated by albite (25 wt. %), actinolite (19 wt. %), chlorite (18 wt. %) and tremolite (16 wt. %) with pyrite (1.3 wt. %) and no measurable carbonates. Reflected light images demonstrate that pyrite is coarser and appears to host magnetite (Figure 20) and in general is less disseminated than in B-Type. Pyrite in this waste type is larger in diameter and shows a more irregular grain morphology but does appear silicate-associated. Based on these observations, the net pH recorded from this kinetic trial would be lower than that for A- and B-Types and given the neutraliser absence and higher content of pyrite, weakly acidic leachates would be expected for the duration of the trial, with a general decline potentially expected overtime (if a significant passivating layer does not form).

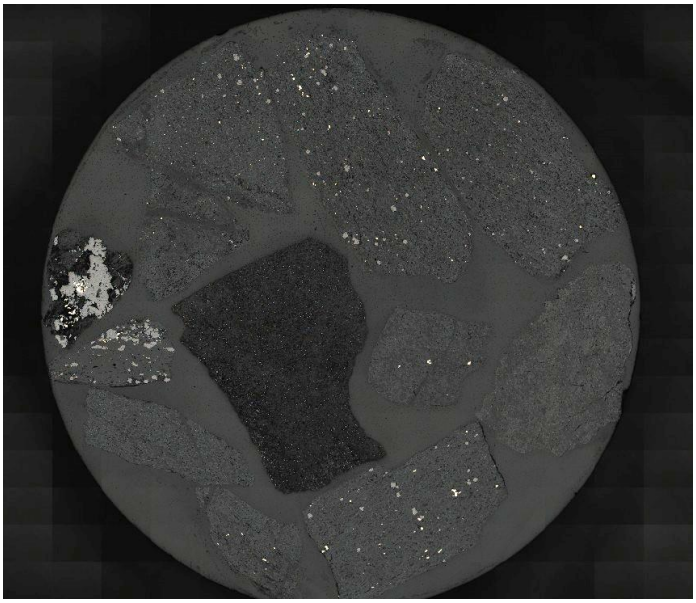

Figure 20. Reflected light image of column feed material collected from LPB. Bright phases are pyrite and magnetite and are visible in the four grains towards the top of the image, where they appear mostly locked in a tremolite/actinolite matrix (diameter of grain mount, 3 cm).

The modal mineralogy as calculated by MLA-SEM was consistent with bulk mineralogy (XRD) measurements and reported feldspar (albite; 20 %), magnesiohornblende (19 %) and chlorite (19 %) as dominating (Figure 21). Edenite (7 %) was again also identified with only 0.7 % pyrite measured, which was lower than estimations based on the bulk mineralogy (Figure 21). Detailed investigations revealed that this is because the pyrite is present as large particles with a *p80* of approximately 550 µm (i.e., 300 µm greater than Types A and B) and the largest particle size also reported as 600 µm (Figure 22). This larger pyrite is expected to be liberated rapidly with these grains chlorite associated (Figure 23) so the kinetic trial leachates may show a general increase overtime, as opposed to having disseminated grains that are differentially liberated and oxidised which may manifest as consistently weak acidic pH conditions. Approximately 10% of pyrite is liberated (Figure 24) so an immediately lower pH would be expected. Smaller pyrite grains are feldspar and chlorite-associated (Figure 23) with both minerals the most pyrite-associated (Figure 24). Based on mineralogical and textural observations, the pH is likely to once again be 'spiky' as part of these larger pyrite grains are liberated and oxidised, the longevity of weakly acid conditions will correlate with the lag-time to a passivating

layer forming. No carbonates are observed at either mineralogical scale, therefore a NAF condition is not expected.

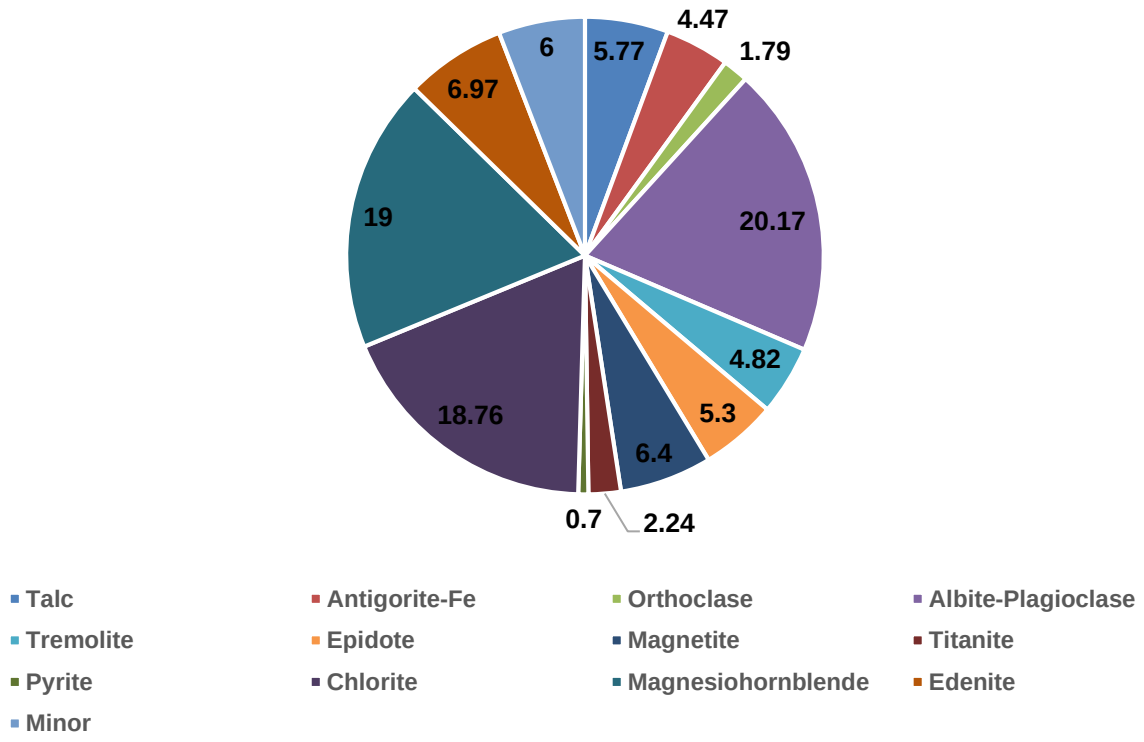

Figure 21. Modal mineralogy as calculated by MLA-SEM for LPD (week 0).

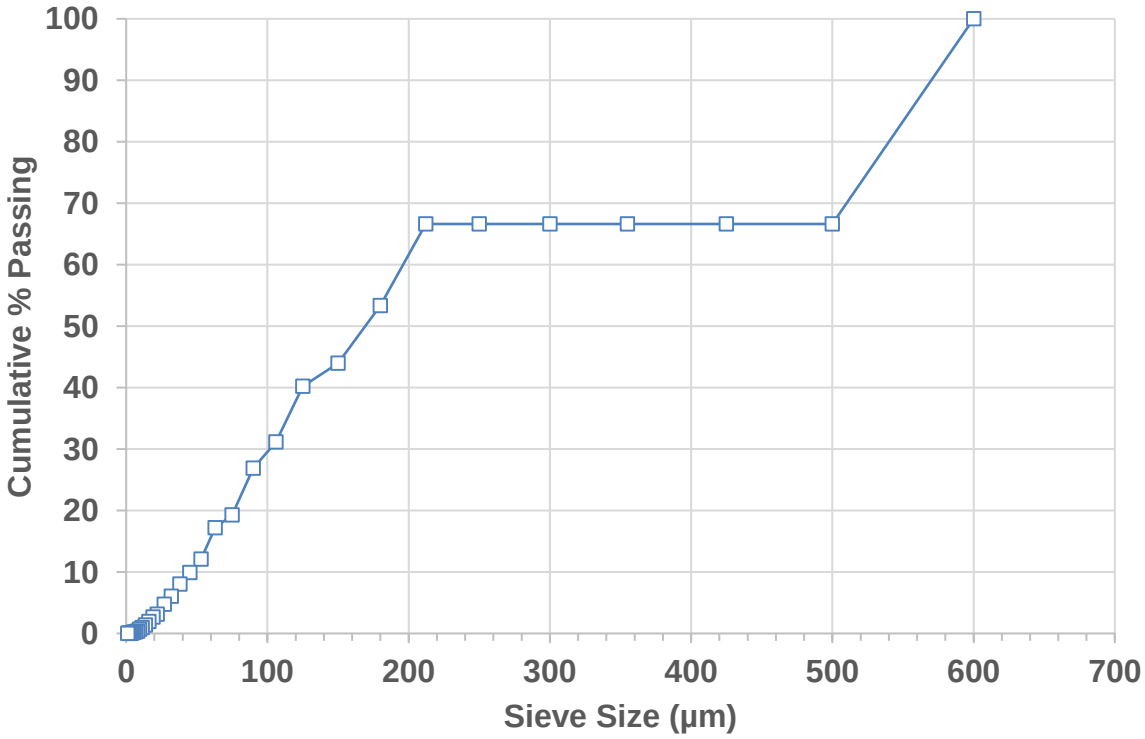

Figure 22. Pyrite grain size distribution (as calculated from MLA-SEM analysis).

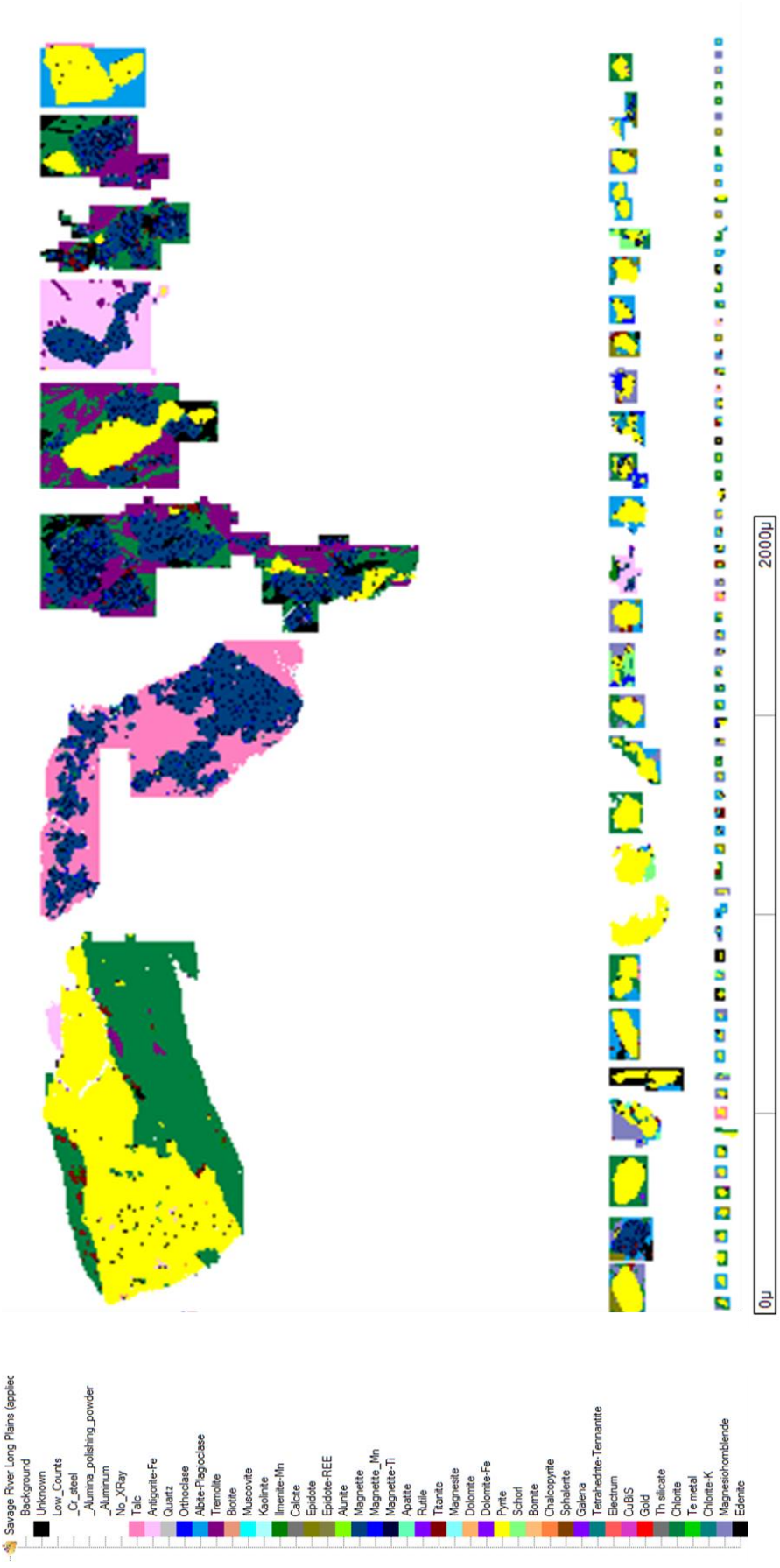

Figure 23. Classified pyrite grains in LPB with their mineral associations shown.

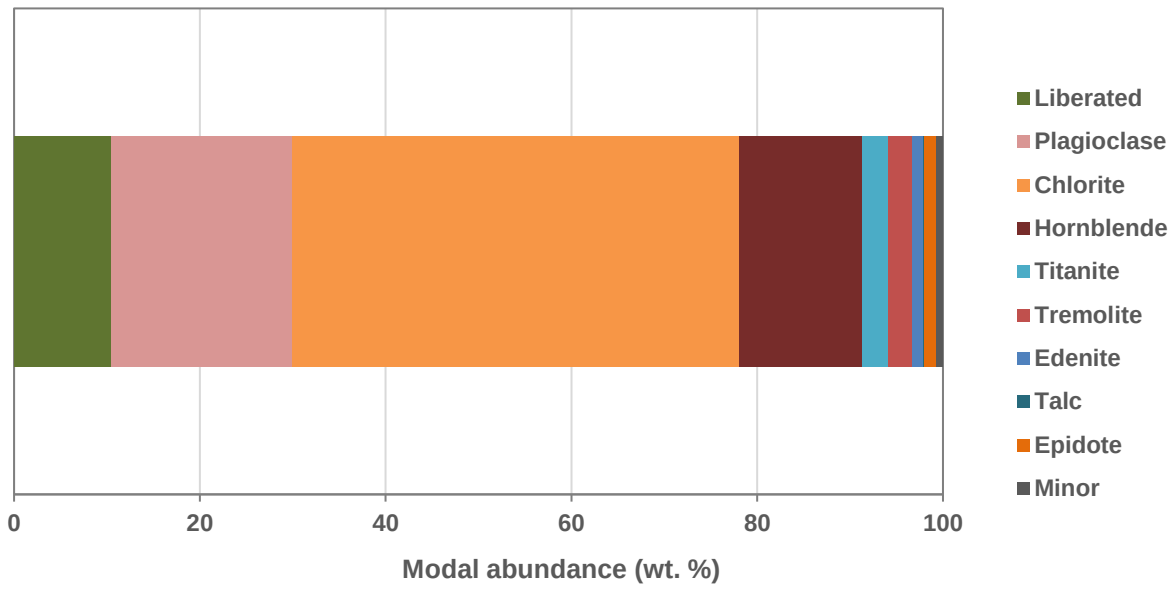

Figure 24. Pyrite locking and liberation of the column B feed materials (week 0, calculated from MLA-SEM analysis).

Kinetic testing of Type D material shows that for the duration of the experiment it remains as NAF (pH 6.9 at week 156) if the cut-off criterion is either set at pH 4.5 or even increased to pH 5.5 (Figure 25). If this were however set at pH 6.5, then the column would be considered as dropping off slightly as measurements in the final 6 months returned several values below this (Figure 25). Indeed, there is a general decreasing trend, but as the final 7 weeks showed progressive pH increases, then an assumption that values are trending towards PAF cannot be made. Instead, based on the MLA data, liberation of pyrite is periodically occurring in the cyclic manner than has been described, the next phase of investigations should focus on SEM work of the reaction products rimming pyrite to determine if indeed stable passivating layers have developed, if this is the case then the column could be considered NAF. The electrical conductivity measurements were relatively consistent and low over the experiment, except for an outlier at Week 10 (696 µs/cm^{-1}) a minimum of 44 µs/cm^{-1} (week 118; Figure 25) suggesting the most cationic activity is in the Type B cell. Sulphate values are also lower than that for the Type B cell with a maximum of 109 mg/L measured at week 34 and 96 mg/L at week 135. Calcium and magnesium are both also low in these leachates (Table 7) except in later weeks, particularly at weeks 131 and 135 with values of 12 mg/L and 27 mg/L measured respectively (Table 7, Figure 26). Despite being the most pyritic sample, the water quality is like the previous columns, with Cu (0.0005 to 0.009 mg/L) and occasionally Al (max: 0.58 mg/L) notably higher, with Cu above the ANZECC (2000) 80% aquatic protection values for most weeks. Occasional measurements of Zn (0.009 and 0.0015 mg/L: weeks 118 and 126), Cd (0.0002 mg/L: weeks 118 and 126) and Co 0.002 mg/L (week 131) were above the instrument detection limit but did not exceed the ANZECC (2000) protection values (data not shown for Cd and Zn). The bulk mineralogy confirms the absence of dolomite and magnesite in this column. Pyrite decreased from 1.3 wt. % to 0.66 wt. % confirming oxidation has taken place. When reacted, passivation has occurred with Zhou et al. (2017) reporting that chlorite can have an active role with pyrite surface passivating layers from the natural dissolution of reactive silicate minerals in real waste rocks, can be preserved in a continuous, coherent, and stable form at pH ≥ 6, and have been found to reduce the pyrite oxidation rate by 50–95%.

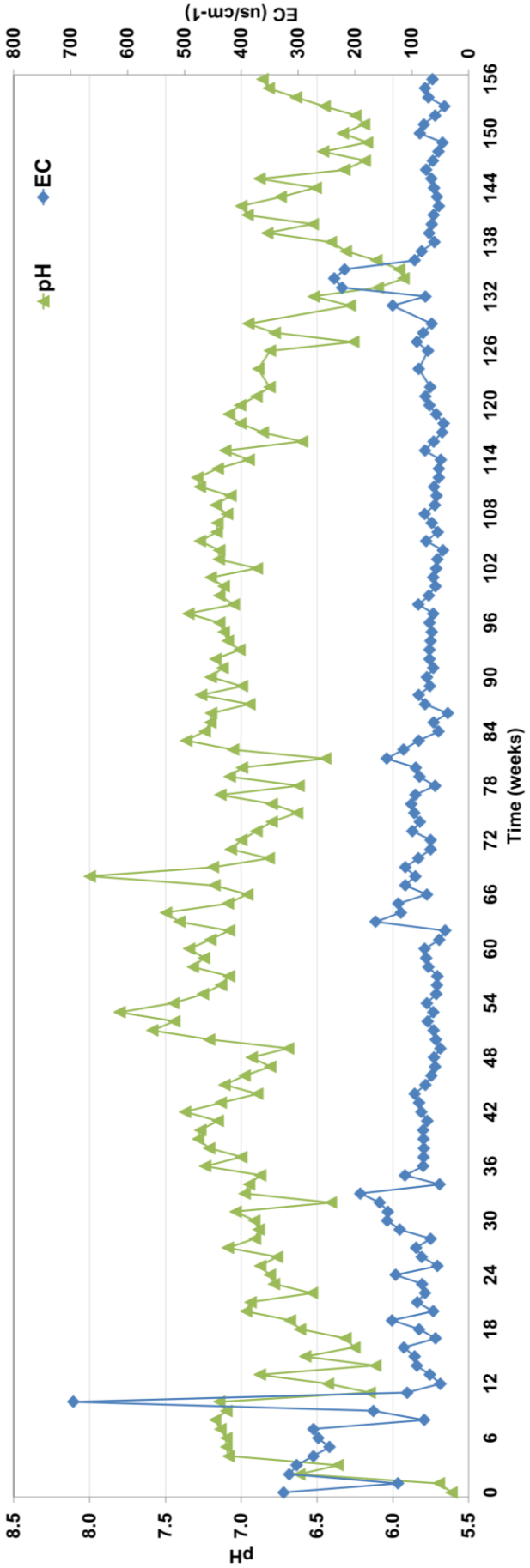

Figure 25. Measurements of pH and EC for Type D waste material (week 0 to 156).

Table 7. Chemistry of Type D waste leachates, measured from week 0 to week 155 (all data in mg/L).

WEEK	SO_4	Al	As	Be	Ba	Co	Cu	Pb	Mn	B	Ca	Mg
ANZECC (2000) 80% protection		*0.15*	*0.14*	*N/D*	*N/D*	*N/A*	*0.0025*	*0.0094*	*3.6*	*N/D*	*N/D*	N/D
0	78	0.005	0.0005	0.002	0.0005	0.006	0.0005	0.092	0.003	0.025	ND	ND
4	7	0.02	0.0005	0.0005	0.0005	0.0005	0.002	0.0005	0.003	0.025	ND	ND
8	25	0.04	0.0005	0.0005	0.001	0.0005	0.01	0.0005	0.024	0.025	ND	ND
12	45	0.04	0.0005	0.0005	0.002	0.0005	0.009	0.0005	0.033	0.025	ND	ND
16	34	0.03	0.0005	0.0005	0.001	0.0005	0.013	0.0005	0.022	0.025	ND	ND
20	44	0.04	0.0005	0.0005	0.002	0.0005	0.009	0.0005	0.032	0.025	ND	ND
24	24	0.05	0.0005	0.0005	0.0005	0.0005	0.012	0.0005	0.014	0.025	ND	ND
30	50	0.005	0.0005	0.002	0.0005	0.009	0.0005	0.026	0.0005	0.025	ND	ND
34	109	0.01	0.0005	0.0005	0.003	0.0005	0.01	0.0005	0.071	0.025	ND	ND
38	27	0.29	0.0005	0.0005	0.002	0.0005	0.004	0.0005	0.014	0.22	ND	ND
42	25	0.02	0.0005	0.0005	0.0005	0.0005	0.009	0.0005	0.014	0.025	ND	ND
46	19	0.03	0.0005	0.0005	0.001	0.0005	0.006	0.0005	0.011	0.025	ND	ND
50	15	0.02	0.001	0.0005	0.0005	0.0005	0.004	0.0005	0.017	0.025	ND	ND
54	23	0.02	0.0005	0.0005	0.002	0.0005	0.005	0.0005	0.011	0.025	3	1
58	22	0.02	0.0005	0.0005	0.001	0.0005	0.012	0.0005	0.011	0.025	3	1
62	31	0.04	0.0005	0.0005	0.001	0.0005	0.014	0.0005	0.007	0.025	3	1
66	27	0.02	0.0005	0.0005	0.001	0.0005	0.002	0.0005	0.02	0.025	3	1
70	37	0.08	0.0005	0.0005	0.001	0.0005	0.011	0.0005	0.029	0.025	5	2
75	31	0.04	0.0005	0.0005	0.002	0.0005	0.005	0.0005	0.02	0.025	4	2
78	19	0.31	0.0005	0.0005	0.002	0.0005	0.002	0.0005	0.011	0.025	3	1
82	24	0.005	0.0005	0.0005	0.151	0.0005	0.006	0.0005	0.028	0.05	8	2
86	13	0.02	0.0005	0.0005	0.144	0.0005	0.005	0.0005	0.018	0.06	5	1
90	21	0.58	0.0005	0.0005	0.131	0.0005	0.007	0.0005	0.026	0.06	6	2
94	21	0.02	0.0005	0.0005	0.120	0.0005	0.007	0.0005	0.023	0.05	6	2
98	22	0.02	0.0005	0.0005	0.118	0.0005	0.007	0.0005	0.024	0.025	6	2
102	22	0.02	0.0005	0.0005	0.122	0.0005	0.004	0.0005	0.023	0.025	6	2
106	16	0.01	<0.001	<0.001	0.001	0.001	0.005	<0.001	0.022	<0.05	4	1
110	16	0.02	<0.001	<0.001	<0.001	<0.001	0.002	<0.001	0.022	<0.05	4	1
114	25	0.02	<0.001	<0.001	<0.001	<0.001	0.002	<0.001	0.03	<0.05	5	1
118	24	0.02	<0.001	<0.001	<0.001	<0.001	0.005	<0.001	0.034	<0.05	5	2
122	22	<0.01	<0.001	<0.001	<0.001	<0.001	0.002	<0.001	0.029	<0.05	5	1
126	22	0.01	<0.001	<0.001	<0.001	<0.001	0.001	<0.001	0.031	<0.05	5	1
131	43	0.02	<0.001	<0.001	0.002	0.002	0.005	<0.001	0.061	<0.05	12	2
135	96	0.014	<0.001	ND	ND	<0.001	0.005	<0.001	0.091	ND	27	4
139	21	0.030	<0.001	ND	ND	<0.001	0.005	<0.001	0.023	ND	7	1
143	17	0.026	<0.001	ND	ND	<0.001	0.007	<0.001	0.026	ND	6	1
147	14	0.044	<0.001	ND	ND	<0.001	0.015	<0.001	0.002	ND	4	<1
151	23	0.015	<0.001	ND	ND	<0.001	0.007	<0.001	0.011	ND	7	1
155	22	0.017	<0.001	ND	ND	<0.001	0.004	<0.001	0.018	ND	7	1

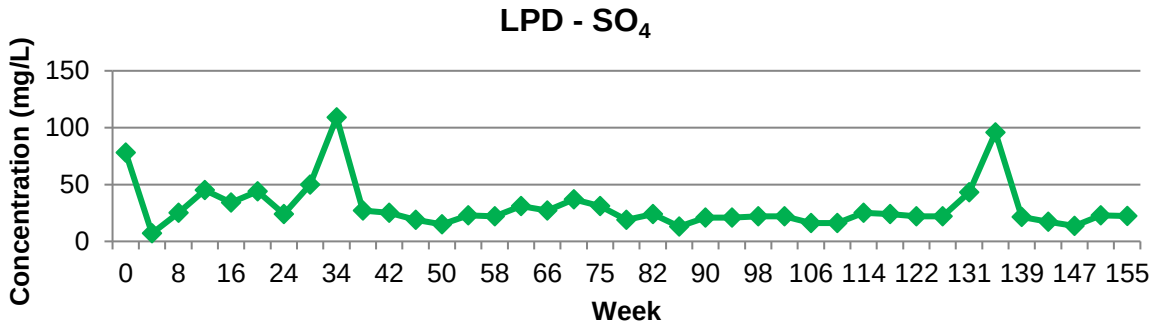
LPD - SO4
Concentration (mg/L)
150
100
50
0
0 8 16 24 34 42 50 58 66 75 82 90 98 106 114 122 131 139 147 155
Week

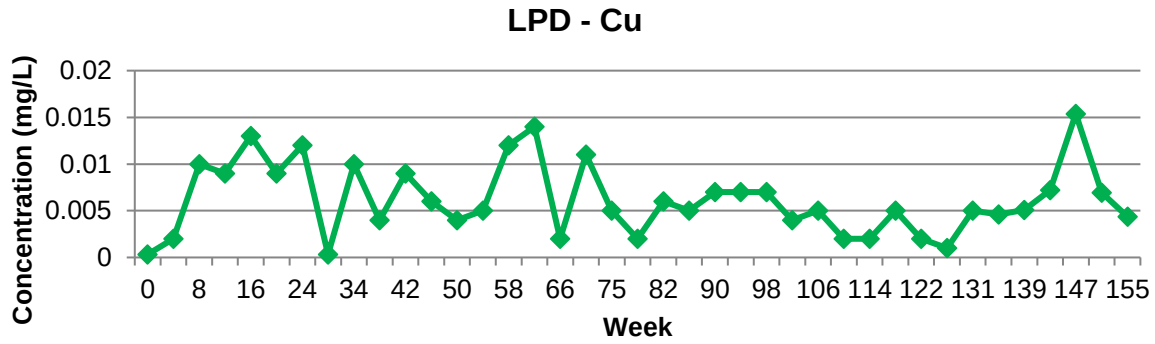
LPD - Cu
Concentration (mg/L)
0.02
0.015
0.01
0.005
0
0 8 16 24 34 42 50 58 66 75 82 90 98 106 114 122 131 139 147 155
Week

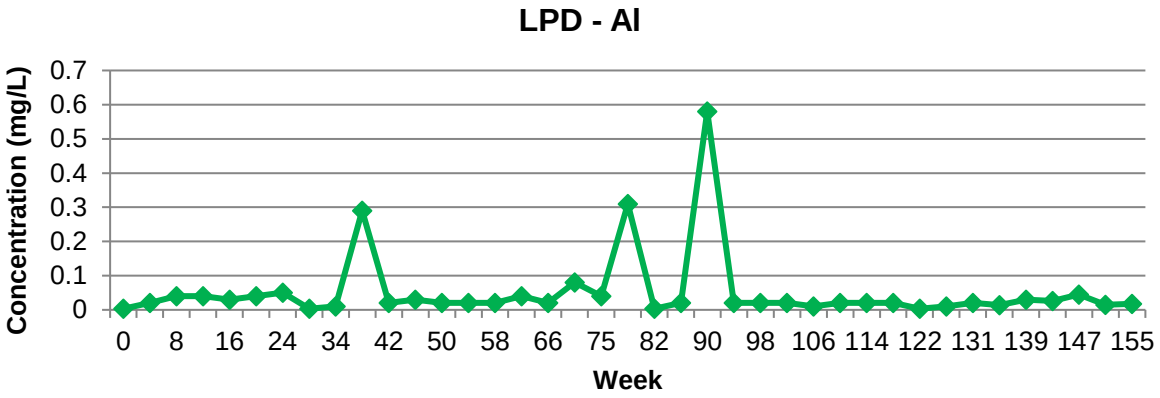
LPD - Al
Concentration (mg/L)
0.7
0.6
0.5
0.4
0.3
0.2
0.1
0
0 8 16 24 34 42 50 58 66 75 82 90 98 106 114 122 131 139 147 155
Week

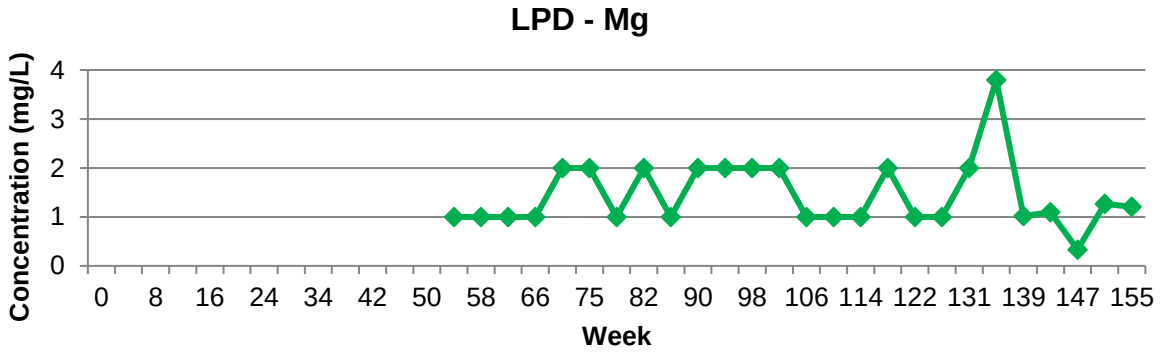
LPD - Mg
Concentration (mg/L)
4
3
2
1
0
0 8 16 24 34 42 50 58 66 75 82 90 98 106 114 122 131 139 147 155
Week

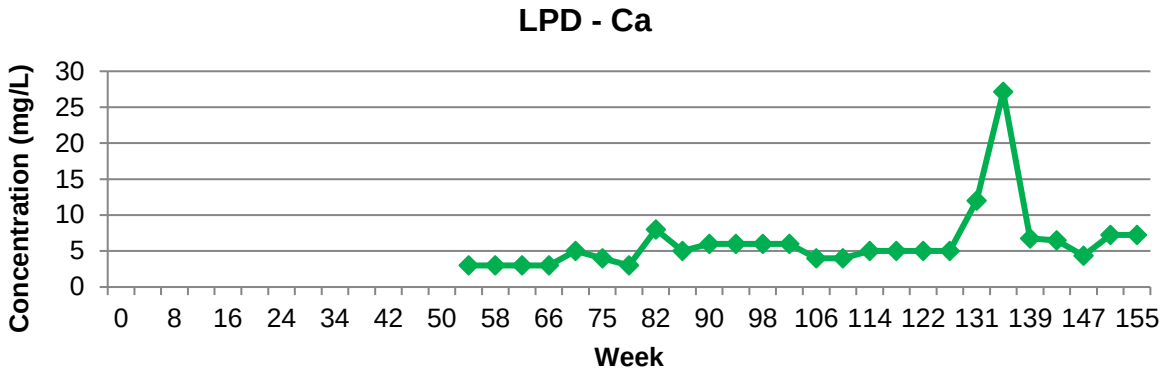

Figure 26. Measurement of Al, Cu, SO_4, Ca and Mg for Type D leachates.

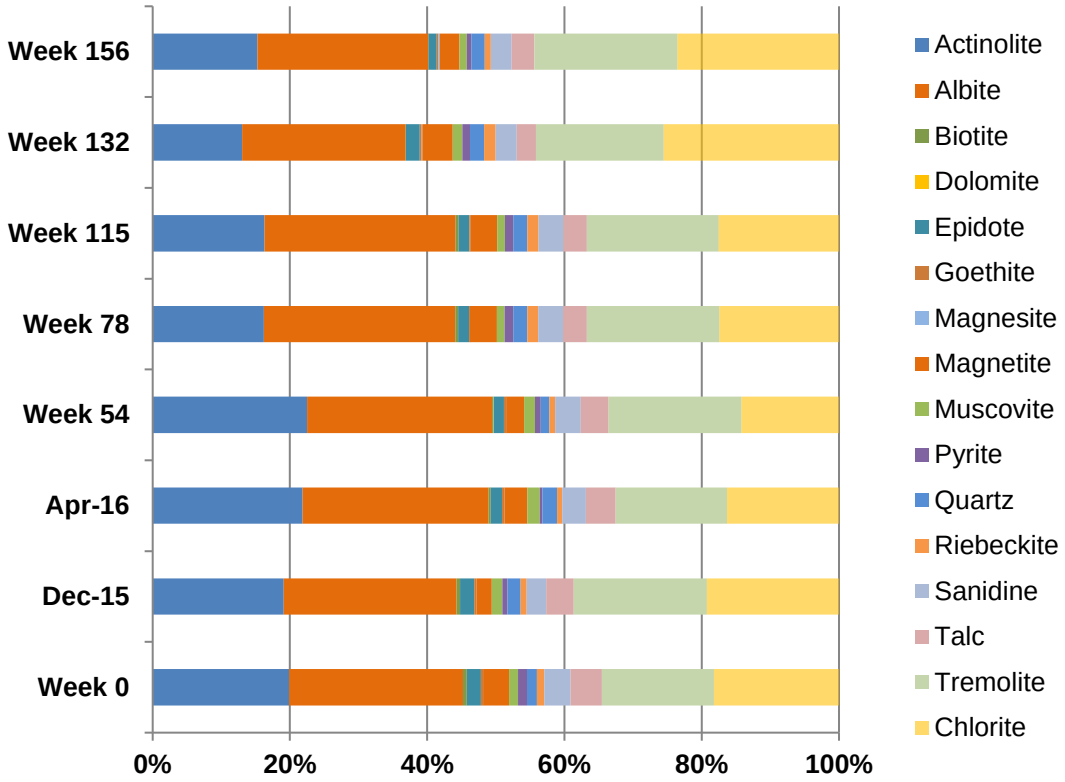

Figure 27. Bulk mineralogy of Type D waste material (measured by XRD).

3.4 Control

The control cell remains as NAF (Figure 28) with a notable outlier at week 122 when a minimum of pH 4.6 was measured, and a maximum of pH 6.9 (weeks 33 and 58; Figure 28). These values (without the afore mentioned weeks) are within the range for deionised water (most weeks water was prepared the morning of irrigation, rather than a day in advance). The electrical conductivity values were very low (< 15 µs/cm^{-1}; Figure 27) except for three outliers which may correlate to an error with the electrode. In the control leachate, both sulphate, Ca and Mg are significantly lower than the waste material cells (< 8 mg/L; Table 8). The reaction vessels were changed in the experiment with fluids recovered from the vessels used from week 106 onwards reporting no Cu, Al, Zn and Mn above detection limit (as in previous weeks).

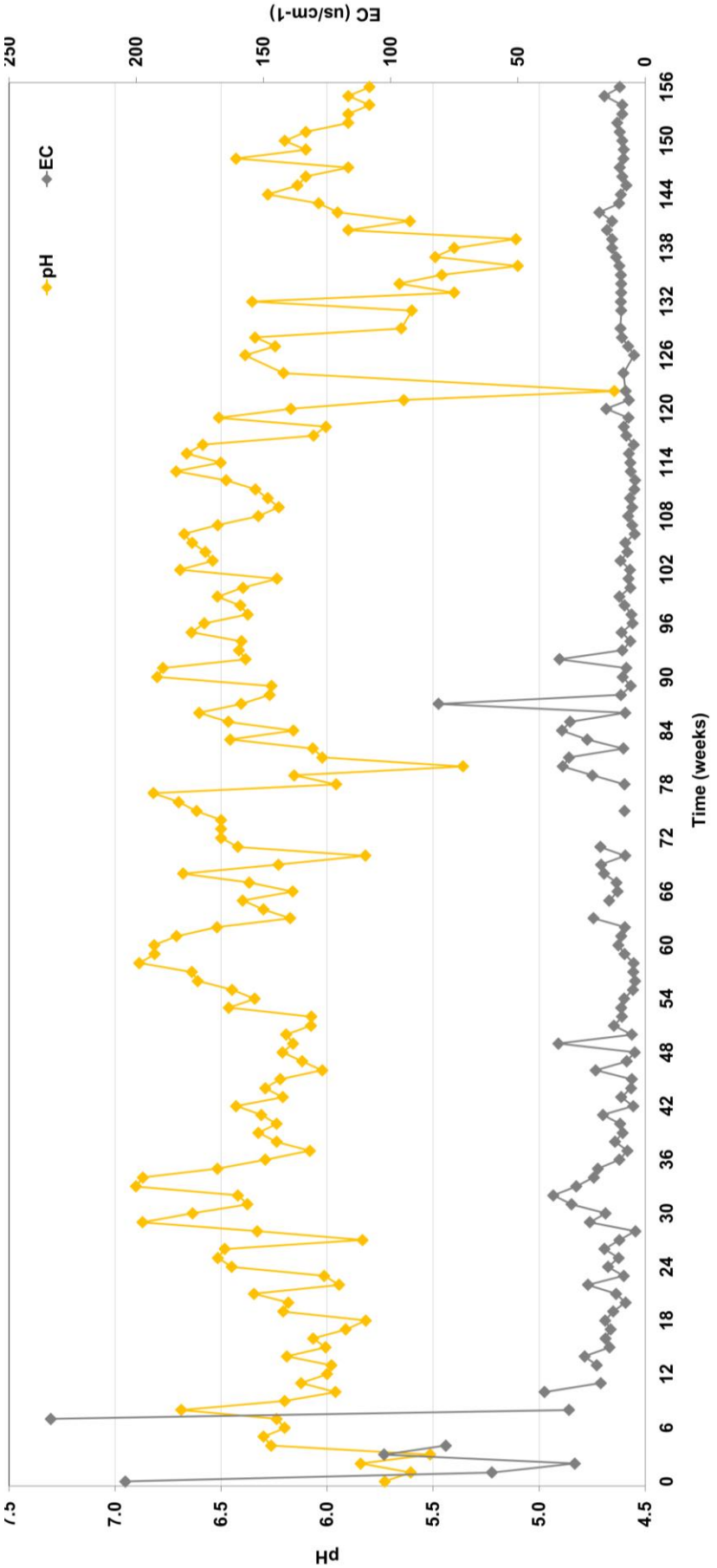

Figure 28. Measurements of pH for the control cell (week 0 to 156).

Table 8. Chemistry of Type control cell leachates, measured from week 12 to week 155 (all data in mg/L).

.	SO_4	Al	Be	Ba	Cr	Co	Cu	Pb	Mn	V	Zn	B	Ca	Mg
12	0.5	0.47	0.0005	0.002	0.002	0.0005	0.012	0.004	0.016	0.005	0.007	0.025	ND	ND
16	0.5	0.26	0.0005	0.0005	0.001	0.0005	0.014	0.0005	0.01	0.005	0.0025	0.025	ND	ND
20	0.5	0.27	0.0005	0.0005	0.0005	0.0005	0.015	0.001	0.01	0.005	0.011	0.025	ND	ND
24	0.5	0.16	0.0005	0.001	0.0005	0.0005	0.04	0.0005	0.006	0.005	0.006	0.025	ND	ND
30	0.5	0.005	0.001	0.0005	0.0005	0.028	0.002	0.009	0.0005	0.01	0.0025	0.025	ND	ND
34	0.5	0.11	0.0005	0.0005	0.0005	0.0005	0.01	0.0005	0.004	0.005	0.0025	0.025	ND	ND
38	0.5	0.64	0.0005	0.002	0.0005	0.0005	0.018	0.0005	0.004	0.005	0.009	0.26	ND	ND
42	0.5	0.05	0.0005	0.0005	0.0005	0.0005	0.008	0.0005	0.002	0.005	0.0025	0.025	ND	ND
46	0.5	0.14	0.0005	0.001	0.0005	0.0005	0.021	0.0005	0.008	0.005	0.011	0.025	ND	ND
50	0.5	0.08	0.0005	0.0005	0.0005	0.0005	0.005	0.0005	0.004	0.005	0.0025	0.025	ND	ND
54	0.5	0.23	0.0005	0.0005	0.0005	0.0005	0.031	0.0005	0.007	0.005	0.006	0.025	<1	<1
58	0.5	0.05	0.0005	0.0005	0.0005	0.0005	0.012	0.0005	0.002	0.005	0.0025	0.025	<1	<1
62	0.5	0.1	0.0005	0.001	0.0005	0.0005	0.038	0.0005	0.036	0.005	0.015	0.025	<1	<1
66	8	0.14	0.0005	0.0005	0.0005	0.0005	0.004	0.0005	0.007	0.005	0.0025	0.025	<1	<1
70	2	0.06	0.0005	0.0005	0.0005	0.0005	0.02	0.0005	0.007	0.005	0.0025	0.025	<1	<1
74	0.5	0.04	0.0005	0.0005	0.0005	0.0005	0.008	0.0005	0.003	0.005	0.0025	0.025	<1	<1
78	2	0.15	0.0005	0.0005	0.0005	0.0005	0.045	0.0005	0.01	0.005	0.0025	0.025	2	<1
82	3	0.02	0.0005	0.160	0.0005	0.0005	0.010	0.0005	0.003	0.005	0.025	0.11	1	<1
86	4	0.03	0.0005	0.164	0.0005	0.0005	0.013	0.0005	0.004	0.005	0.038	0.07	1	<1
90	3	0.02	0.0005	0.184	0.0005	0.0005	0.006	0.0005	0.003	0.005	0.028	0.11	<1	<1
94	2	0.03	0.0005	0.123	0.0005	0.0005	0.016	0.0005	0.003	0.005	0.038	0.06	1	<1
98	2	0.02	0.0005	0.133	0.0005	0.0005	0.016	0.0005	0.003	0.005	0.027	0.06	<1	<1
102	2	0. 03	0.0005	0.122	0.0005	0.0005	0.007	0.0005	0.002	0.005	0.030	0.025	<1	<1
106	<1	<0.01	<0.001	<0.01	<0.001	<0.001	<0.001	<0.001	<0.001	<0.01	<0.005	<0.05	<1	<1
110	<1	<0.01	<0.001	<0.01	<0.001	<0.001	<0.001	<0.001	<0.001	<0.01	<0.005	<0.05	<1	<1
114	<1	<0.01	<0.001	<0.01	<0.001	<0.001	<0.001	<0.001	<0.001	<0.01	<0.005	<0.05	<1	<1
118	<1	<0.01	<0.001	<0.01	<0.001	<0.001	<0.001	<0.001	<0.001	<0.01	<0.005	<0.05	<1	<1
122	<1	<0.01	<0.001	<0.01	<0.001	<0.001	<0.001	<0.001	<0.001	<0.01	<0.005	<0.05	<1	<1
126	<1	<0.01	<0.001	<0.01	<0.001	<0.001	<0.001	<0.001	<0.001	<0.01	<0.005	<0.05	<1	<1
131	<1	<0.01	<0.001	<0.01	<0.001	<0.001	<0.001	<0.001	<0.001	<0.01	<0.005	<0.05	<1	<1
135	<1	0.018	ND	ND	<0.001	<0.001	0.006	<0.001	0.004	<0.01	0.067	<0.05	<1	<1
139	<1	<0.01	ND	ND	<0.001	<0.001	0.002	<0.001	<0.001	<0.01	0.005	<0.05	<1	<1
143	<1	0.018	ND	ND	<0.001	<0.001	0.005	<0.001	<0.001	<0.01	0.004	<0.05	<1	<1
147	<1	ND	ND	ND	ND	ND	ND	ND	ND	ND	ND	<0.05	<1	<1
151	<1	0.017	ND	ND	<0.001	<0.001	0.008	<0.001	<0.001	<0.01	0.006	<0.05	<1	<1
155	<1	0..020	ND	ND	<0.001	<0.001	0.006	<0.001	<0.001	<0.01	0.067	<0.05	<1	<1

3.5 Comparison of cells

A comparison of the pH data from each cell is shown in Figure 29 and confirms that all cells remain as NAF at week 156 if a cut-off criterion of pH 4.5 (for PAF or NAF) is used. If pH 6 was instead used, then Type D is currently above, but if this was pH 6.5 then over the last six months, several values below this were measured. As reported in the Interim Reports, Type A contains the highest reservoir of carbonate and is overall the least acid forming, however in this past six months of testing similar NAF values are reported from the Type B cell, showing that when dealing with low-carbonate, low-sulphide waste, silicate buffering (via chlorite most likely) is contributing to keeping the pH in the NAF realm, likely through surface reactions causing or enhancing the formation of passivating layers.

A comparison of sulphate over time (Figure 30) confirms that Type A is the least acid generating, but surprisingly, Type B consistently returns the highest sulphate concentrations suggesting that sulphides contained in this group are more liberated than Type D (which contains a higher bulk-contents as indicated by the XRD analyses) which automated mineralogical work demonstrated. It is not known if another Type D sample would have returned a similar result as a bulk assessment of the column feed has not been undertaken. It is suggested that a rock scanning technique (i.e., Corescan) is undertaken and new algorithms to identify sulphides are applied (Cracknell et al., in review) as this may reveal the grain size and therefore an understanding if the rest of the pyrite is like the MLA examined Type D material. If so, then the observations made in this report are correct. The interpretations made in this report support the hypothesis that passivating layers enhanced by the presence of chlorite are forming on sulphides and this will continue long-term as chlorite is in abundance and whilst it is stated as being reacting in accordance with Sverdrup (1990) enough of this material will remain across the three waste types. The role of antigorite should also be considered in broader environmental terms too, because this mineral is part of the serpentine group and can fix CO_2 (Li and Hitch, 2017). Pyrite oxidation generates sulphuric acid which is an activator for this process when serpentine group minerals are involved.

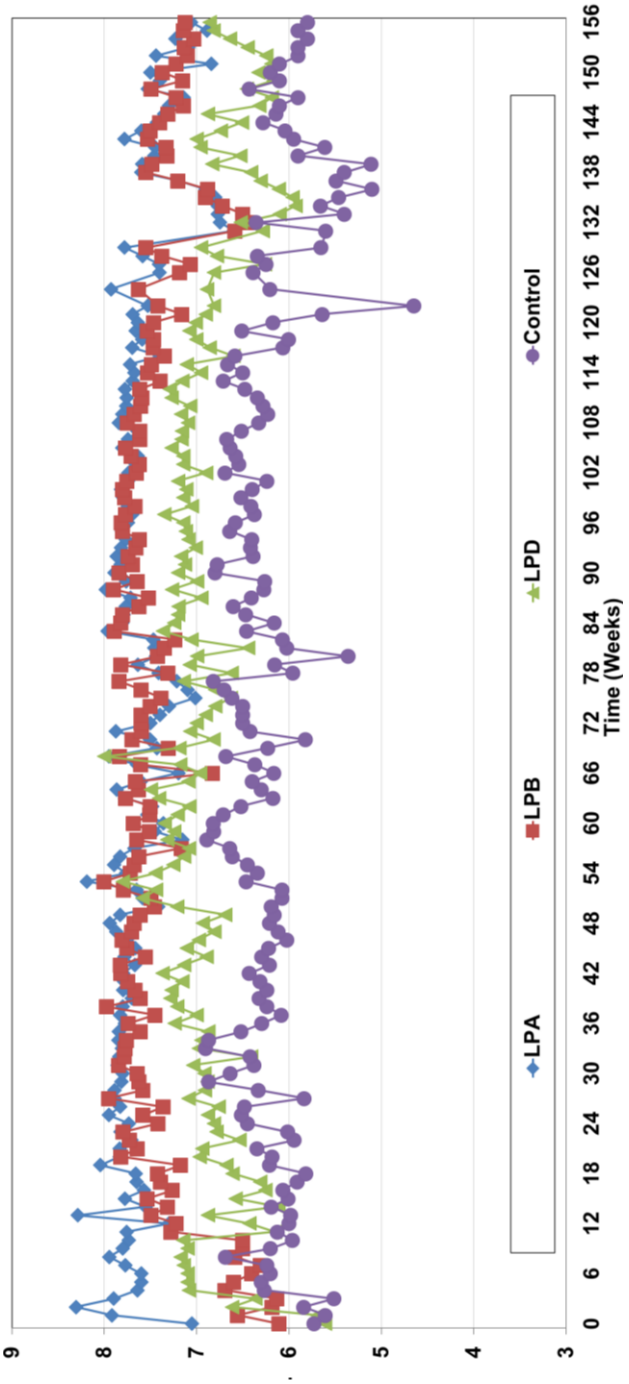

Figure 29. Comparison of leachate pH derived from Type A, B and D wastes and the control (week 0 to 156).

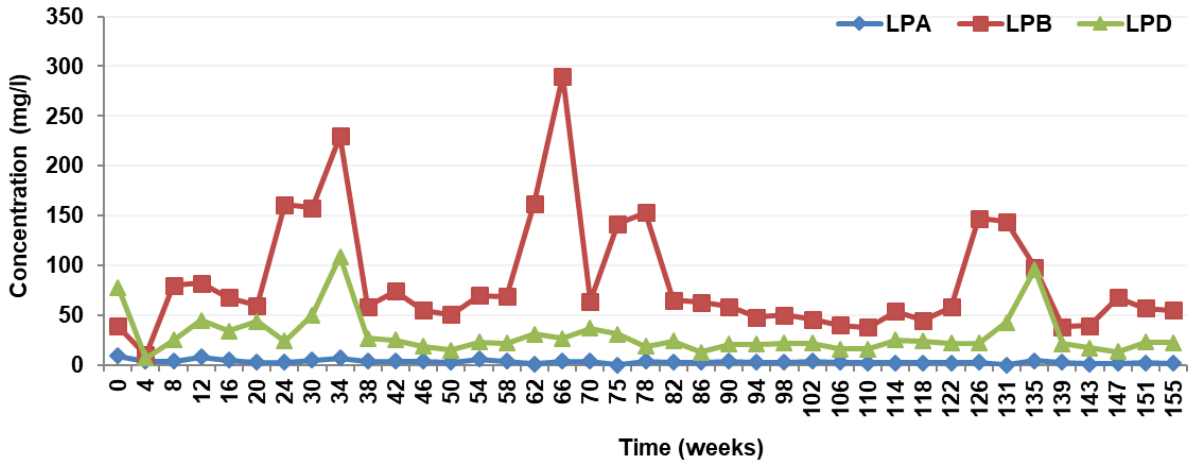

Figure 30. Comparison of sulphate (mg/L) measured in Type A, B and D leachates (week 0 to 155).

A comparison of Ca + Mg over time (from week 54 onwards- not measured before this; Figure 31) shows that the highest alkali earth cation concentrations come from the Type B cell, despite there being a much lower content of dolomite and magnesite relative to Type A indicating that its source is/are other mineral phases (e.g., secondary sulphates such as gypsum, or silicates including epidote: $Ca_2Al_2(Fe^{3+};Al)(SiO_4)(Si_2O_7)O(OH)$; talc: $H_2Mg_3(SiO_3)_4$ or $Mg_3Si_4O_{10}(OH)_2$; or chlorite: $(Mg_5Al)(AlSi_3)O_{10}(OH)_8$)). Whilst these silicate mineral phases would not be immediately obvious candidates thought to undergo significant weathering in this type of experiment (maximum temperature 40 °C), if they are fractured and indeed, well liberated, then it is possible that localised weathering is occurring, and due to the localised nature, secondary reaction products are not detected by XRD (e.g., iron oxides).

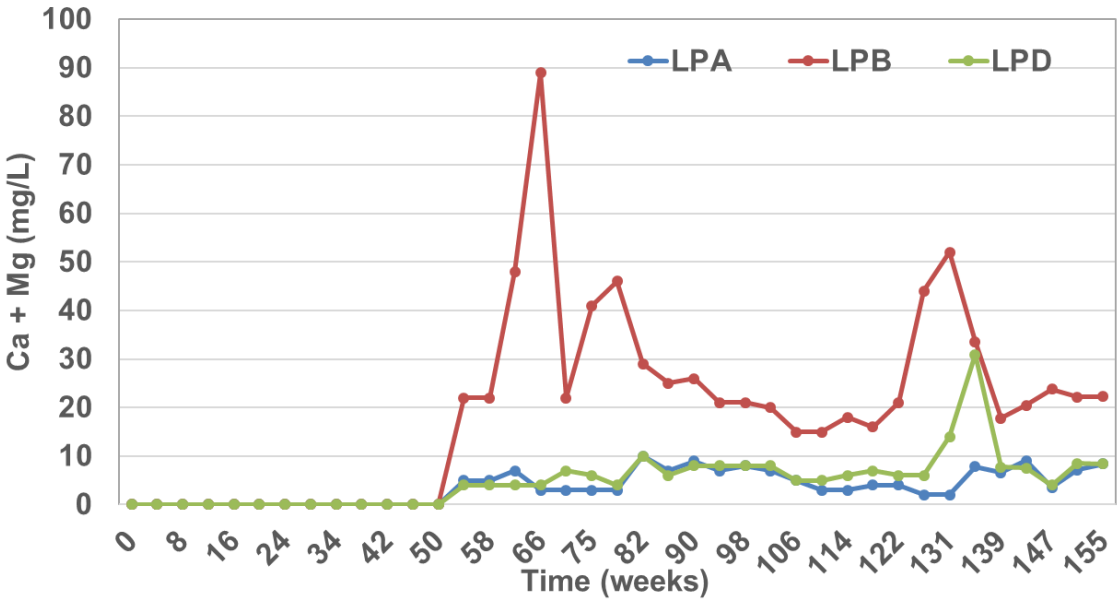

Figure 31. Comparison of calcium + magnesium (mg/L) measured in Type A, B and D leachates (week 54 to 155).

Static characterisation of the column feed and end of experiment samples is shown in Table 9. USGS FLT pH values are high for all three samples (pH 8.5 to 9.09) potentially correlating to the dissolution of transient mineral phases (e.g., Al or Ca hydroxides, gypsum) and carbonates for Type A and Type B. NAG pH values provide a more realistic snapshot of these samples with Type A considered

NAF at both the start and end of the experiment, LPB reported as PAF at the start and NAF at the end, due to the likely formation of passivating layers which are interpreted as impervious to hydrogen peroxide attack (this has not been researched and could be an area for further investigation). Type D classifies as PAF both at the start and at the end (though note, the pH value is 0.3 units higher at the end). This highlights the importance of conducting a column feed automated mineralogy investigation as texturally, the pyrite is encapsulated, and this sample is NAF, as the kinetic leachates have confirmed for the 156 weeks of testing. If no MLA investigation had been performed, this cell may have run for a longer time (i.e., several more years) and we predict that based on the MLA data, it would still be reported as NAF. To confirm this, more MLA investigations should be conducted on representative samples of this waste type, to validate these results the answer is not necessarily to establish several more Type D columns. The leachates from these experiments show that Zn and Ni were both higher at the start than end for Type D, but Cu remained broadly similar at both times. Elements such as As, Cd and Pb are very low risk and some Co may elute from Type D on sulphide oxidation. The NAG leachate from Type B reports values an order of magnitude higher for several elements and correlates to the lower NAG pH value reported for this sample at the start. Thus, at the start of pyrite oxidation, some risk is posed, so the critical step is ensuring the rapid formation of the passivating layer, thus taking measures to ensure the development of this is recommended (i.e., always blend A-Type with B so an active source of alkalinity is present to kick start this; Zhou et al., 2017).

Table 9. USGS field leach test and NAG pH values for LPA, LPB and LPD column feed and end of experiment materials.

Sample	Paste pH	NAG pH
LPA: Start	8.53	7.29
LPB: End	8.62	7.94
LPB: Start	8.81	3.37
LPB: End	8.98	7.17
LPD: Start	9.09	3.24
LPD: End	8.8	3.54

Table 10. Element concentrations (mg/L) measured in NAG leachates for LPA, LPB and LPD column feed and end of experiment materials.

	LPA Start	LPB Start	LPD Start	LPA End	LPB End	LPD End
Ba137(LR)	0.67	2.18	0.53	0.38	0.14	0.14
Pb208(LR)	0.01	0.08	0.12	0.00	0.00	0.02
S32(MR)	59.28	622.65	643.88	45.59	162.33	474.16
V51(MR)	0.26	1.65	1.35	0.24	0.83	1.04
Cr52(MR)	2.75	1.15	1.10	0.02	0.17	0.10
Mn55(MR)	1.06	6.65	6.44	0.13	0.13	4.23
Fe56(MR)	0.46	0.88	0.80	0.21	0.16	1.35
Co59(MR)	0.00	5.62	5.15	0.00	0.00	3.38
Ni60(MR)	1.56	20.42	16.50	0.33	0.37	1.48
Cu63(MR)	0.16	8.93	4.73	0.05	0.04	5.26
Zn66(MR)	0.53	24.77	15.93	0.14	0.32	0.48
As75(HR)	0.02	0.00	0.00	0.00	0.00	0.00
Se82(HR)	0.00	0.41	0.00	0.20	0.09	0.38

4.0 OUTCOMES

This section gives a list of outcomes from this study. However, these are based on the analyses of a limited number of waste rock samples.

1. All waste types (A, B and D) are NAF from weeks 1 to 156 if a PAF/NAF cut-off of pH 4.5 (or even 5.5) is used. Relative to ANZECC (2000) aquatic protection values (80% level) Cu is the most significant contaminant for concern and continues to persist in latter weeks for all columns. Al is also identified as being elevated and should also be flagged for management and control measures put in place for its management as high concentrations can impact on aquatic life.

2. Investigations into the nature of the passivating layers likely forming on exposed or semi-liberated pyrite should be commissioned as this is the key to controlling AMD elution in these waste materials. Once identified, experiments to test its robustness should be designed to work out its durability (i.e., can it withstand a range of temperatures, pH, Eh and salinity conditions?).

3. Blending of Type A and Type B to form this passivating layer should be investigated, and indeed, how such blending may influence the lag-time to the formation of this layer.

4. Determining if the antigorite (serpentine) identified in Type D is a significant mineral at Long Plains and if it is, calculating if its theoretical capacity to fix atmospheric CO_2 should be investigated further. If it is present in significant quantities than ensuring it is activated for fixing CO_2 should be part of the waste handling flowsheet as this will give Grange Resources additional 'green credits'.

5. It is recommended that Grange always perform bulk mineralogical and textural work on column feed materials prior to any kinetic trial as without this, the chemical results are not easy to explain and forecasting the behaviour of the waste materials is compromised.

6. Further analytical results (as part of an ATSE funded project) will be made available to Grange Resources once they are collected and processed. This will include laser ablation ICPMS data on the sulphides and other key silicate phases in these samples to examine the Cu contents.

REFERENCES

Brough, C., Strongman, J., Bowell, R., Warrender, R., Prestia, A., Barnes, A., Fletcher., J. 2017. Automated environmental mineralogy; the use of liberation analysis in humidity cell testwork. *Minerals Engineering*, In Press. http://dx.doi.org/10.1016/j.mineng.2016.10.006

Cracknell, M., Parbhakar-Fox, A., Jackson, L., Savinova, E. Automated acid rock drainage indexing from drill core imagery. Submitted to *Minerals, September 2018.*

GHD, 2014. Savage River Waste Management Concept Designs for Future Waste Disposal, 83 pp.

Li, Jiajie & Hitch, Michael. (2017). A Review on Integrated Mineral Carbonation Process in Ultramafic Mine Deposit. Geo-Resources Environment and Engineering. 2. 10.15273/gree.2017.02.027.

Miller, S.D., Stewart, W., Rusdinar, Y., Schumann, R., Ciccarelli, J.M., Li, J., Smart, R. 2010. Methods for estimation of long-term non-carbonate neutralisation of acid rock drainage, *Science of the Total Environment*, 408: 2129-2135.

Munksgaard, N.C., Lottermoser, B.G. 2011. Fertilizer Amendment of Mining-Impacted Soils from Broken Hill, Australia: Fixation or Release of Contaminants? *Water, Air and Soil Pollution*, 215: 373-397.

Noble, T., Lottermoser, B.G., Parbhakar-Fox, A, 2016. Evaluation of pH testing methods for sulfidic mine waste. *Mine Water and the Environment*, 35: 318-331.

Parbhakar-Fox, A., Lottermoser, B.G., Bradshaw, D.J. 2013. Evaluating waste rock mineralogy and microtexture during kinetic testing for improved acid rock drainage prediction. *Minerals Engineering,* 52: 111-124.

Qian, G., Schumann, R.C., Li, J., Short, M.D., Fan, R., Li, Y., Kawashima, N., Zhou, Y., Smart, R., Gerson, A.R. 2017. Strategies for reducing acid and metalliferous drainage by pyrite surface passivation. Minerals, 7(3), 42; doi: 10.3390/min7030042.

Smart, R., Skinner, W.M., Levay, G., Gerson. A.R., Thomas, J.E., Sobieraj, H., Schumann, R., Weisener, C.G., Weber, P.A., Miller, S.D., Stewart, W.A. 2002. ARD test handbook: Project P387, A prediction and kinetic control of acid mine drainage, Melbourne, Australia, AMIRA, International Ltd.

Stewart, W.A., 2005. Development of Acid Rock Drainage Prediction Methodologies for Coal Mine Wastes, PhD Dissertation, University of South Australia.

Sverdrup, HU, 1990. The Kinetics of Base Cation Release Due to Chemical Weathering. Lund, Sweden: Lund Univ. Press. 246 pp.

WHO Aquatic Protection Values. https://www.environment.gov.au/system/files/resources/53cda9ea-7ec2-49d4-af29-d1dde09e96ef/files/nwqms-guidelines-4-vol1.pdf

Zhou, Y., Short, M.D., Li, J., Schumann, R.C., Smart, R., Gerson, A., Qian, G 2017. Control of acid generation from pyrite oxidation in a highly reactive natural waste: A laboratory case study. *Minerals*, 7, 89; doi:10.3390/min7060089.